Technical Summary Report for Period
27 June 1966 to 27 March 1967

SOLAR-RADIATION-INDUCED DAMAGE
TO OPTICAL PROPERTIES OF
ZnO-TYPE PIGMENTS

NAS 8-18114   June 1967

FACILITY FORM 602

N68 - 14171
(ACCESSION NUMBER)

90
(PAGES)

CR-61429
(NASA CR OR TMX OR AD NUMBER)

(THRU)

(CODE)
33
(CATEGORY)

FOREWORD

This report was prepared by the Lockheed Palo Alto Research
Laboratory of the Lockheed Missiles & Space Company, for the
George C. Marshall Space Flight Center of the National Aero-
nautics and Space Administration. The work was performed
under contract NAS 8-18114. The contract was administered by
the Research Project Laboratory of Marshall Space Flight
Center with Mr. G. M. Arnett as Contract Officer.

The authors gratefully acknowledge the advice, encouragement,
and continued interest of Mr. G. M. Arnett, Dr. R. Lal,
Mr. E. R. Miller, Mr. W. C. Snoddy. and Mr. G. Heller of
the Research Projects Laboratory.

This Technical Summary Report describes work performed from
27 June 1966 to 27 March 1967.

PERSONNEL

The following personnel are responsible for the work described in this report:

M. E. Browne   A. F. Sklensky
K. F. Cuff   N. L. Thomas
S. A. Greenberg   E. R. Washwell
H. F. Mac Millan

The program was carried out under the direction of S. A. Greenberg. Experimental studies of ESR effects in irradiated ZnO were performed by M. E. Browne and N. L. Thomas. The balance of the experimental studies on sintered and single crystal ZnO were conducted by H. F. Mac Millan and A. F. Sklensky. Preparation and characterization of samples were performed by H. F. Mac Millan, A. F. Sklensky, and E. R. Washwell. Theoretical analysis and review and evaluation of experimental data were conducted in part by all personnel with primary efforts by S. A. Greenberg and K. F. Cuff.

ABSTRACT

Results are reported on investigation of the mechanism of solar
radiation damage to the optical properties of ZnO pigment. Solar
U-V irradiation of particulate ZnO in vacuum produces significant
decreases in reflectance in the visible region adjacent to the funda-
mental band-edge and in the I-R region between 0.8 and 2.8 μ.
Emphasis has been placed on identification of the processes of
I-R degradation using experimental evidence from ESR, electrical
conductivity, and spectral reflectance measurements performed
during U-V irradiation in vacuum and recovery from degradation
in oxygen. The results have led to formulation of a degradation
model which qualitatively accounts for all of the observed data.
With reasonable confidence the UV-induced I-R absorption is
attributed to excitation from bound donor states associated with
oxygen vacancies resulting from lattice photolysis. The induced
visible absorption is tentatively assigned to states or to lattice
strain resulting from diffusion of surface zinc to sites in the
particle bulk.

CONTENTS

ILLUSTRATIONS

Section 1

INTRODUCTION

Operational spacecraft performance is strongly dependent on the degree to which components can be maintained within their designed temperature limits. Since the exchange of radiant energy between the vehicle and its environment determines the temperature, the optical properties of the exterior surfaces necessarily play a critical role in temperature control. Design requirements frequently necessitate the use of a surface with a low ratio of solar absorptance, α_s, to emittance, ϵ. The type of low α_s/ϵ surface most commonly employed on spacecraft is a white coating composed of a high refractive index pigment dispersed in a binder with a lower refractive index. These surfaces are generally susceptible to damage by natural or induced radiation in space, resulting in increased vehicle temperatures as a larger fraction of the incident solar energy is absorbed by the degraded coating (Refs. 1−14).

These changes in thermal control properties have emphasized the necessity for obtaining better insight into the nature of the damage mechanisms in thermal control coating systems. Knowledge of the damage mechanisms would greatly simplify the problem by providing a rational basis both for the design of environmental tests and for interpretation of the resulting data. Ultimately, such knowledge would guide materials specialists in the development of optimum materials.

The complexity of both the pigment-binder systems and the total space environment precludes a comprehensive investigation of the combined aspects of space radiation induced degradation. However, of all sources of radiation encountered in space, the U-V portion of the solar spectrum is the most important source of damage to low α_s/ϵ surfaces. In regard to the coating systems, changes in the optical properties of the pigment portion generally dominate, so that investigations can be restricted to that component. Zinc oxide has been selected as the subject of the investigations on the

1

basis of its being representative of a class of white pigments in use in promising thermal control coatings as well as being relatively well characterized in terms of optical, electrical, and transport properties.

The investigation then, has been devoted to an experimental study of the optical behavior of particulate samples of ZnO. Such samples have been exposed in vacuum to radiation of wavelengths between 0.2 and 2.6 μ. Parameters varied in both initial exposures and studies of damage reversibility were flux density, spectrum, and time of exposure. Selected exposures were performed in which the bidirectional spectral reflectance of the sample was monitored during exposure (in situ). The in situ measurements provide the key to comprehensive detailed knowledge of optical damage to particulate samples. Photoconductivity measurements have been used to characterize the damage processes and to correlate optical and electrical properties in ZnO. Electron spin resonance (ESR) techniques have been useful in characterizing radiation induced defects. In addition, single crystals of ZnO have been irradiated, in an attempt to ascertain the relative importance of surface and bulk damage processes.

A parallel theoretical and experimental program to describe the pertinent bulk and surface properties of ZnO has been carried out. The goal of these parallel efforts has been to formulate a comprehensive explanation of phenomena observed in the particulate samples. Selected measurements of optical properties of ZnO single crystals were performed to formulate a coherent picture of ZnO optical behavior. These efforts have resulted in a refinement of the degradation model for ZnO formulated under Contract NAS 8-11266 (Ref. 15).

2

Section 2

BACKGROUND

The program discussed in this report continues the scope of investigations initiated under NASA contract NAS 8-11266 (Refs. 15 – 17). The major conclusions deriving from that effort are summarized below:

- An apparatus for performing in situ bidirectional reflectance measurements was constructed and successfully operated.

- The initial reflectance spectra of the pressed and sintered particulate samples were quite similar to those of ZnO-pigmented thermal control paints, over the wavelength range 0.27 to 2.5μ (except for binder absorptions in the infrared).

- Solar-radiation-induced reduction in reflectance of the particulate samples over the same wavelength range was similar to that observed for ZnO paints.

- The ZnO optical property changes observed in the visible region of the spectrum appear to be connected with the loss and gain of oxygen by the ZnO.

- Solar-radiation-induced reduction in reflectance spectra of particulate samples recovers upon exposure to air.

- The solar-radiation-induced reduction in the reflectance for visible energy is apparently initially generated near the surface, whereas reduction in I-R reflectance appears to be more of a bulk phenomenon.

- The effect of sample temperature on the degradation of particulate ZnO indicates that the visible damage is enhanced at elevated temperatures, while the I-R damage is relatively insensitive to temperature.

- The effects in the particulate sample reflectance spectra produced by (1) solar-radiation in vacuum, (2) high sample forming pressure, and (3) sintering in vacuum were similar enough to suggest one predominant underlying cause.

- Sintering in vacuum appears to produce free Zn at the surface of the particulate samples.

3

- Conclusive evidence for the photodesorption and adsorption of oxygen on particulate ZnO was obtained.
- The information available on diffusion rates in ZnO and the complex diffusion conditions near the surface prevent quantitative prediction of the time dependence of the damage processes.
- A band structure for ZnO was derived in a preliminary manner by the method of corresponding states.
- U-V exposures with <u>in situ</u> bidirectional reflectance measurements play a crucial role in the construction and evaluation of a model for the mechanism of optical damage to ZnO.
- A working model for solar radiation induced damage to the optical properties of ZnO was formulated.

During the course of that program, the primary characterization of the solar-radiation-induced change to ZnO was made in terms of the changes in optical properties of the samples. The relationships existing between the ZnO employed in that work and the material employed in thermal control paints was of particular interest. Although no binder materials were included with the pressed and sintered samples, the reflectance spectra were found to be quite similar, over the wavelength range of 0.27 to 2.5μ, to those of ZnO paints. This observation, in connection with the findings that the average particle sizes of the original ZnO powder and the sample compacts were approximately the same, indicated that the sample preparation procedures did not alter the properties of the material appreciably. Therefore, it is to be expected that, exclusive of binder effects and pigment-binder interactions, the damage processes observed in these studies are similar to those occurring in ZnO paint systems. The relative simplicity of the pure pigment system has led to a better understanding of those processes characteristic of the pigment, without the added complexities of pigment-binder interactions.

One unifying trend in the data was apparent throughout the experimental studies: many of the changes in the optical properties of ZnO appeared to be connected with the loss and gain of oxygen by the ZnO lattice. This was borne out not only by the results of irradiation in vacuum and air, but also by the changes in optical properties induced by sintering in vacuum. The results emphasized the need for <u>in situ</u> measurements

4

of sample reflectance, since recovery and bleaching effects greatly limited the quantitative significance of post-exposure reflectance measurements.

A major portion of the effort in that program was devoted to developing the in situ bidirectional reflectance measurement and U-V exposure apparatus and to learning the strengths and limitations of this new analytical tool. Excessive quantitative importance was not attributed to the preliminary in situ data accumulated in the initial study. However, the trends and qualitative behavior observed were extremely significant. Because of the complications involved in observation of the spectral and temporal dependence of recovery, in situ measurements were shown to be mandatory for accurate determinations of the kinetics of damage and recovery.

A working model of the degradation of the optical properties of ZnO by U-V radiation was formulated on the basis of a critical evaluation of the extensive literature on ZnO and on the results obtained under NAS 8-11266. The model is predicated on an initial description of a ZnO particle in an oxygen atmosphere. The surface (Fig. 1) takes on a negative charge due to electrons bound to the oxygen atoms chemisorbed at the surface. The potential barrier produced in the surface region is such that electrons will be repelled and holes will be attracted to the surface within the space charge layer. The volume near the surface will therefore be a depletion region since ZnO is an n-type semiconductor.

When U-V radiation of energy greater than the intrinsic energy gap (3.2 eV) is incident on the sample, electron-hole pairs are created within the bulk of the crystal or particle; the absorption depth for the radiation is $0.1\,\mu$ or less. The electrons have difficulty in getting to the surface but the holes will be accelerated to the surface by the action of the strong electric field in the space charge region. The holes recombine with the O^- at the surface and change the oxygen from the chemisorbed to the physically adsorbed form which then can leave the surface with relative ease. The activation energy for physical adsorption is roughly 0.05 eV. This process results in oxygen leaving the surface which becomes Zn rich. Furthermore, this Zn rich surface layer gives a positive contribution to surface charge, thus decreasing the band bending and potential

5
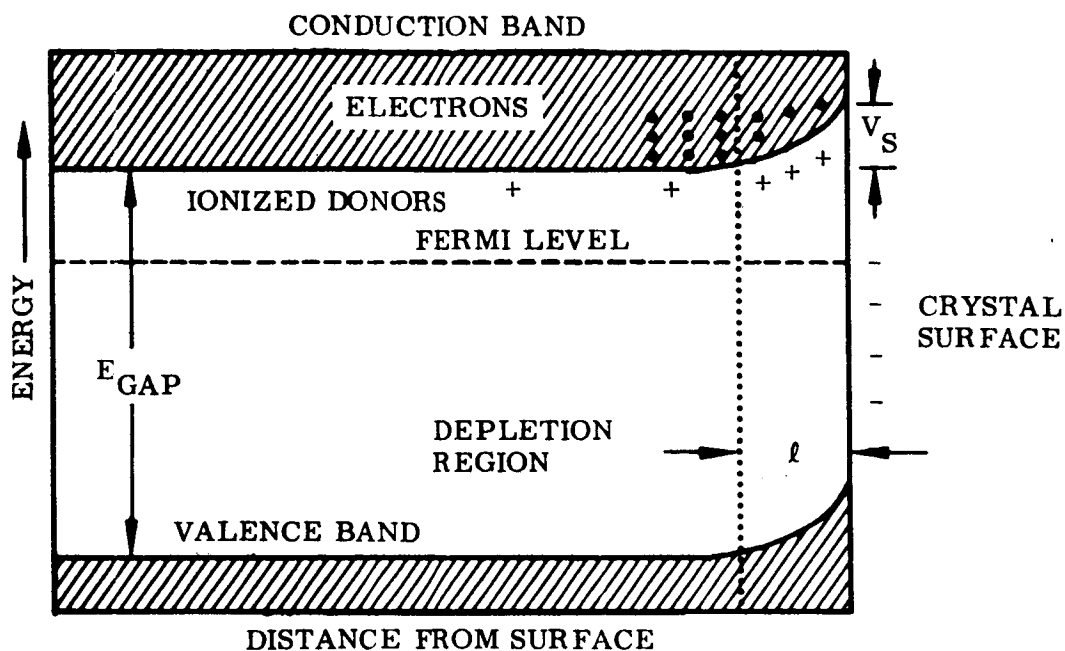
Fig. 1 Surface Band Bending in Depletion Region

barrier at the surface. As the degradation proceeds the surface charge will tend to change to a net positive charge and the bands at the surface will begin to bend down (Fig. 2). Under this condition the holes have a retarding potential at the surface to overcome and the rate of charge neutralization slows down severely. Thus the degradation process (loss of oxygen) proceeds initially at a rate largely determined by the rate of evolution of adsorbed oxygen and eventually at a rate limited by the arrival of holes through the retarding potential of the positive surface charge.

With this general trend outlined, the next step is to ascertain what changes produced by this oxygen loss manifest themselves as the permanent damage observed in various spectral regions by the reflectivity from pigments. Two general consequences are expected to result from the oxygen loss. Changes in the band-bending can be expected to modify the availability for optical absorption of the defect states already present in the ZnO crystallites because of changes in the relative positions of the defect states and the Fermi level. Diffusion of defects and impurities is also expected to occur and would give rise to additional absorption.

6

CONDUCTION BAND

ELECTRONS

ENERGY →

FERMI LEVEL

E_{GAP}

ACCUMULATION REGION

VALENCE BAND

V_S

+
+
+
+

CRYSTAL SURFACE

ℓ

DISTANCE FROM SURFACE
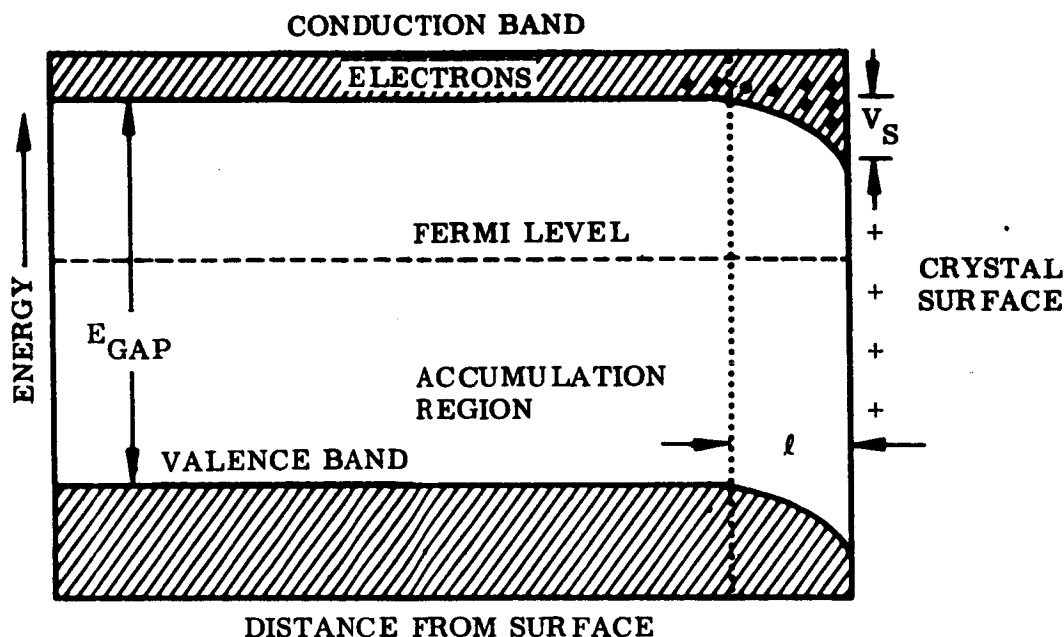
Fig. 2 Surface Band Bending in Accumulation Region

There was insufficient information at the time to specify the exact nature of the defect states giving rise to the optical absorption observed in the damaged ZnO pigments. However, some comments as to the defects to be expected were made. With the loss of oxygen from the surface both interstitial Zn and oxygen vacancies can be expected to diffuse into the material. It was pointed out that the problem of predicting diffusion rates in the pigments is very difficult. Even if the diffusion rates of the defects were well-known in single crystals — and there is much contradiction in this area — the complexities of the interactions near the surface of the crystallites prevented realistic estimates of these diffusion rates in the pigments. However, assuming interstitial Zn and oxygen vacancies as the defects some of the consequences were indicated. Interstitial Zn provides rather shallow (~ 0.05 eV) donor states and oxygen vacancies provide donor states ~ 0.8 eV below the conduction band (Fig. 3). At the densities of defects expected in the degraded material these levels are expected to be considerably broadened; thus if these levels were present, significant absorption should be observed in the material for photon energies from ~ 2.1 to 3.2 eV; that is, over the wavelength interval of 0.38 to 0.6 μ.

7
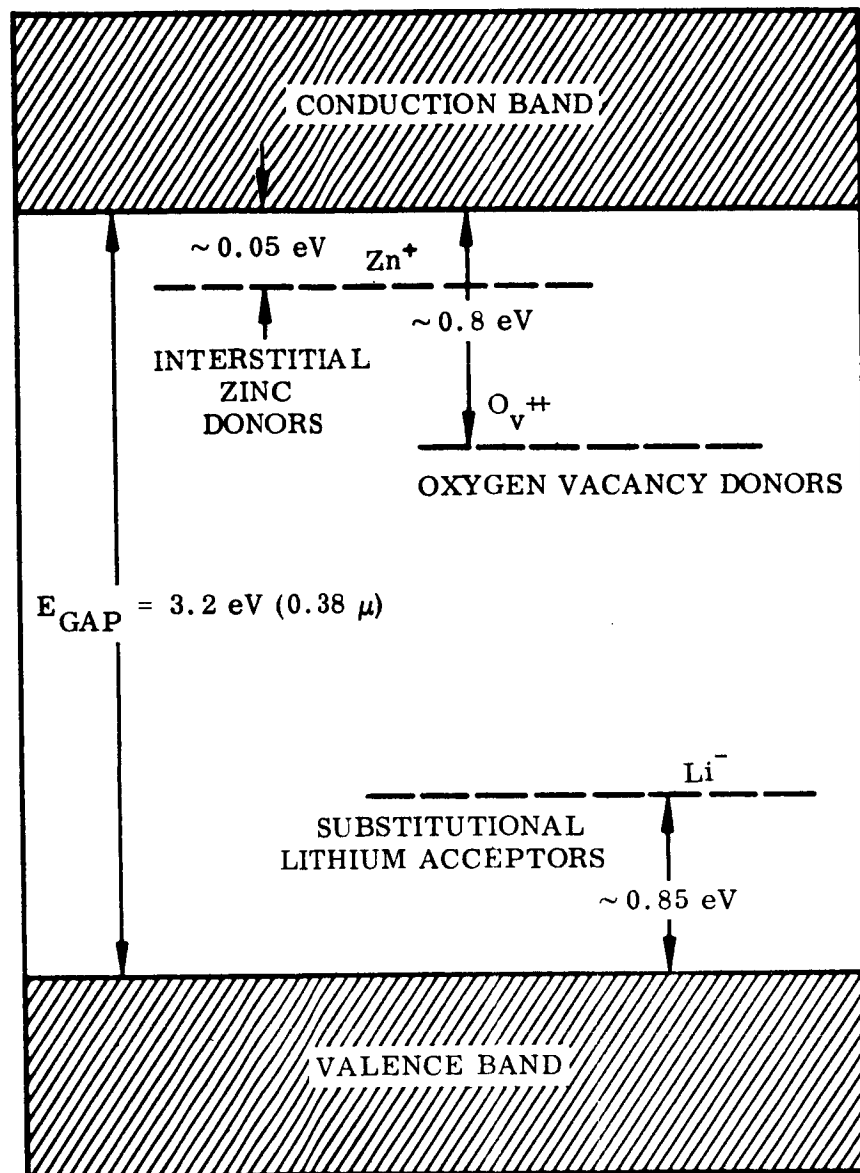
Fig. 3 Bulk Impurity States

It was suggested that in the infrared two types of absorption could occur as a result of the degradation. First, the existence of levels with energies up to 1 eV below the conduction band could provide absorption for wavelengths longer than $1\,\mu$. Also, since Zn interstitial and oxygen vacancies are donors, the electron density in the bulk of the crystal could be increased, which would result in increased free carrier scattering absorption. It was emphasized the data available did not allow an

8

unambiguous assignment of the levels giving rise to the optical absorption observed in the degraded material.

There was one consequence of the degradation model which was pointed out. The model would predict that the photodesorption rate of oxygen from the surface should be significantly retarded if the Fermi level in the bulk of the crystallites could be lowered sufficiently. This should occur regardless of whether the Fermi level is pinned at the surface state energy. If it is not pinned and the Fermi level can be lowered beneath the surface state energy the surface charges will be depleted of electrons (Fig. 4) and the photodesorption rate should diminish. If the Fermi level is pinned at the surface (which will occur at large surface coverage) a lower Fermi level in the bulk of the crystallites will decrease the band bending. It could even cause the bands to turn down at the surface depending upon the relative level of the bulk Fermi level and the surface state energy. This decreased band bending also tends to decrease the photodesorption rate.

The postulated degradation model has served as a point of departure for the program reported here. The greatest emphasis of this program has been toward characterization of the solar-radiation-induced absorption in the I-R spectrum of ZnO, and the refinement of the damage mechanism.

The in situ measurement of spectral reflectance has been the primary tool for this study. In conjunction with optical property measurements, electrical conductivity and ESR techniques have been used for diagnostic purposes. Only through correlation of the optical, electrical, chemical, and transport properties of ZnO can a complete description of the solar-radiation-induced damage to ZnO pigments be achieved.

9

CONDUCTION BAND

FERMI LEVEL

E_{GAP}

O^- CRYSTAL
SURFACE
STATE
FILLED

VALENCE BAND

CONDUCTION BAND

E_{GAP}

FERMI LEVEL

O CRYSTAL
SURFACE
STATE
EMPTY

VALENCE BAND
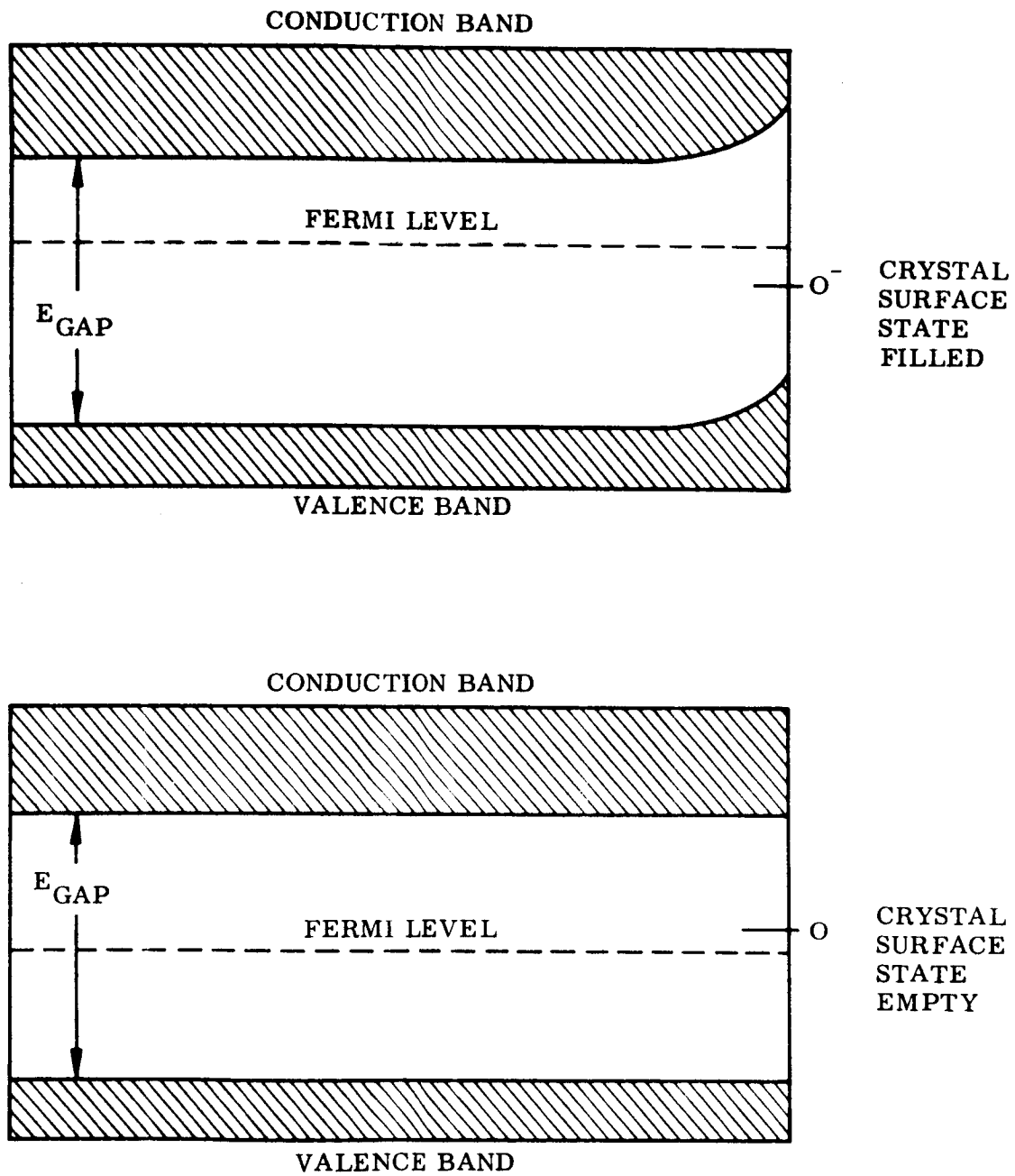
Fig. 4 Effect of Fermi Level on Surface State Occupancy

10

Section 3
EXPERIMENTAL TECHNIQUES

All data presented in this report were obtained from one or more of six pieces of experimental equipment. Since four of these have been built or modified at Lockheed, they will be described in detail below. The remaining two are standard items and will only be described in general terms.

The two standard items are a Gary Model 14 recording spectrophotometer with integrating sphere attachment and a Gier-Dunkle heated-cavity reflectometer. The former is capable of recording reflectance or transmission spectra from 0.3 to 2.5 μ. The latter is capable of transmission or absolute reflectance measurements from 2 to 25 μ. Both spectrophotometers are used in conjunction with U-V irradiation equipment to evaluate the transmission or reflectance of samples at various stages of U-V damage and recovery from damage.

All U-V radiation was produced by a 1-kW PEK Labs A-H6 mercury-argon high-pressure arc lamp. This source is rich in short wavelength light, as the well-known mercury emission spectrum predominates. The lamp is a poor solar simulator, which is of considerable importance for engineering work, as will be shown in Sec. 5.3, but is irrelevant for work described in this report.

3.1 BIDIRECTIONAL REFLECTANCE U-V EXPOSURE APPARATUS

This equipment has been described in detail in Ref. 17. This equipment was conceived, designed, and built at Lockheed. It is capable of making in situ optical and electrical measurements under virtually any gaseous environment at pressures ranging from 10^{-8} Torr to atmospheric, and at sample temperatures from that of liquid nitrogen to 500° F. The optical measurements may be made in either the

11

transmission or reflection mode, utilizing light pipes. The former mode has been used for single crystals and the latter for sintered powder samples. The spectral region covered is between 0.35 and 2.4 μ. The electrical measurements are of conductivity and use a standard 4-point probe technique. Such measurements have been made on the sintered powder samples. The vacuum in the chamber is produced with a VacIon pump after sorption roughing. The sample temperature is controlled continuously over the necessary range through the use of a combination of a heater and liquid nitrogen. Room temperature is achieved by the use of water flowing through the sample holder. The chamber contains a liquid nitrogen cold trap and numerous screens (held at various potentials with respect to ground) across the ion pump mouth to reduce the effects of contamination (Fig. 5).

The radiant source for spectral bidirectional reflectance measurements is a 1000-W tungsten lamp located in an air-cooled housing at the left of Fig. 5. The lamp output is focused at the end of one light pipe (at the left in Fig. 5) and interrupted by a 20-cps synchronous motor-driven chopper. The quartz light pipe penetrates the vacuum chamber wall and projects the chopped energy onto the sample. Energy reflected from the sample and striking the end of the second light pipe is collected and transmitted to a collimating lens, then passed through a monochromator. The monochromator is a Bausch and Lomb Grating Monochromator with interchangeable gratings and variable slits, which can be used over the range 0.18 to 3.2 μ. The spectral bidirectional reflectance is determined by detecting the spectral energy reflected from the sample and collected by the receiver pipe, $E(\lambda)$. Then the source pipe is rotated about its axis so as to view the receiver pipe directly with the sample table withdrawn. The spectral energy $E_0(\lambda)$ detected in the latter alignment is termed the reference energy. The reference energy is measured each time a bidirectional spectrum is measured in order to account for any changes in tungsten lamp output, detector sensitivity, or transmittance of the optical components. The ratio of the reflected spectral energy to the reference spectral energy, $E(\lambda)/E_0(\lambda)$, is proportional to the spectral bidirectional reflectance.
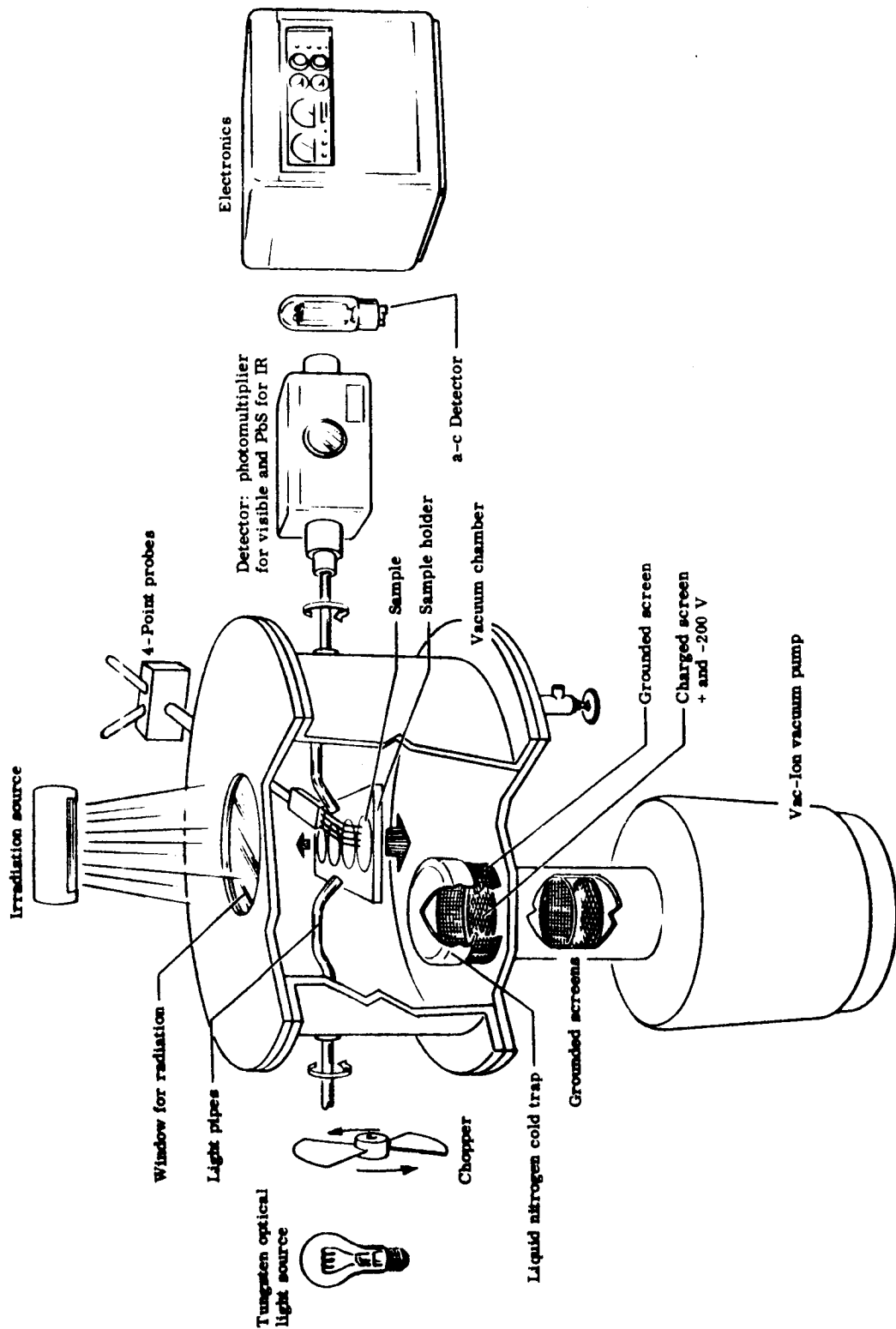
Fig. 5 Bidirectional Reflectance U-V Irradiation Device

13

The absolute value of this ratio has no significance because in the detection of both the reflected and the reference energy, no attempt is made to evaluate the losses through the optical system. However, these losses are a constant fraction of the detected signals, and therefore the ratio of the reflected and reference signals will be proportional to the spectral bidirectional reflectance. This ratio, herein termed the spectral bidirectional reflectance, is in turn related to the spectral normal reflectance by a proportionality factor. This factor is established by normalizing the initial spectral bidirectional reflectance so that it equals the initial spectral normal reflectance of the sample as measured on a Cary Model 14 spectrophotometer with an integrating sphere attachment. The in situ bidirectional reflectance data are presented in this way even though the bidirectional reflectance is generally not equal to the directional reflectance for a real surface. This form of presentation depends on the validity of the assumption that the ratio of reflected energy to reference energy will continue to be proportional to the directional reflectance of a material as it is exposed to vacuum U-V irradiation and to post-irradiation recovery effects.

In normalizing the initial bidirectional reflectance so that it equals the initial normal reflectance, it is not necessary to use a different proportionality factor for each wavelength at which measurements are made, but it has been found that one proportionality factor is required for the wavelength region in which the photomultiplier detector is used and another (usually slightly different) is required for the wavelength region in which the photoresistor detector is used. The need for two factors is apparently due to the differences in variation of photosensitivity over the two detector surfaces.

Transmission spectra of single crystals are obtained by placing the single crystals over holes in the sample holder, rotating one light pipe. and measuring the intensity of the light transmitted through each crystal in turn. As in the case of reflectance measurements, the ratio of the sample reading to that of the reference is taken. and this ratio normalized to a transmission spectrum obtained from the Cary Model 14.

The source of U-V radiation is a PEK Labs A-H6 mercury argon high-pressure arc lamp. The intensity on the samples is varied by varying the distance from the lamp

14

to the sample. The spectrum of the light striking the samples may be varied by placing filters over the samples. In practice, this is done by fixing the filters with respect to the chamber so that they cover the desired sample(s) when the sample holder is in its normal irradiation position. It is possible to filter three of the four sample positions, each with a different filter. In situ optical spectra are then taken by translating the sample holder in the normal way to place the sample of interest beneath the light pipes. The irradiation source must be extinguished during this process so that the samples will receive no unfiltered radiation.

The vacuum in the irradiation chamber is produced by first roughing with a cryogenic sorption pump and then, when the pressure becomes low enough, switching to the ion pump. It has been found that during the initial start-up period the ion pump gives off an effluent of charged particles. Screens have been placed as shown in Fig. 5 in an attempt to reduce this effluent. Finally, a 4-point probe technique is used to measure conductivity. The circuit is shown in Fig. 6 and the probes are constructed as shown in Fig. 7. The voltage supply impresses a potential across the sample, causing a
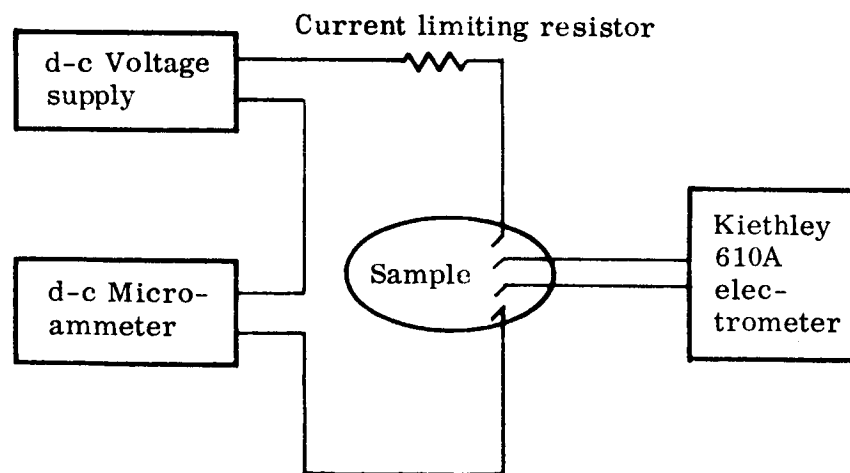
Fig. 6 Conductivity Measurement Circuit

15

U-V radiation

Light pipe
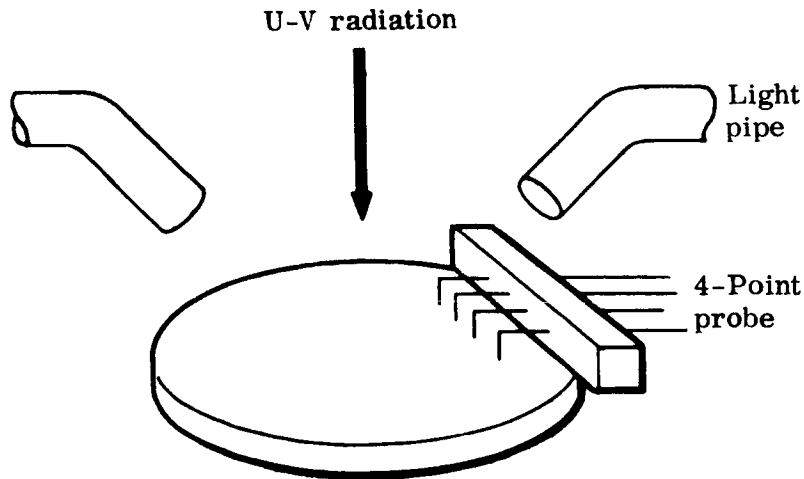
4-Point probe

Fig. 7 Four-Point Probe Configuration

current to flow between the outer probes. The current in turn causes a potential difference across the voltage probes in the center. This voltage must be measured without drawing any current, so that no voltage drop is incurred across the contact resistance between the sample and voltage probes. A potentiometer should be used for this, but it was found that the Kiethley electrometer introduced no error into the readings.

3.2 NORMAL REFLECTANCE U-V EXPOSURE APPARATUS

A second device for making in situ optical measurements has been designed and built by Lockheed. It utilizes the integrating sphere attachment on the Cary Model 14 for making optical measurements, rather than the light pipes used in the bidirectional reflectance apparatus. The relevant difference between these two devices is that the start-up glow discharge of the ion pump is eliminated in the normal reflectance apparatus.

16

Figure 8 is a schematic representation of this device. The chamber is small enough, and the valving is such that it is possible to leave the ion pump on at all times. When it is desired to change samples, the high vacuum portion is sealed off, the rest of the chamber brought to atmospheric pressure, the samples changed, and the sample chamber roughed down once again. Since the sample area is small as compared to the rest of the chamber, it possible to open the valve to the high-vacuum portion, when the sample portion has been roughed to a sufficiently low pressure, without causing the ion pump to revert to a start-up glow discharge and consequently produce charged particles.

Optical measurements are made with this device as follows. The samples are held very close to the inside surface of the Suprasil window through which they are irradiated and measured. The window, and thus each sample, is placed against the port in the integrating sphere in the Cary spectrophotometer. A normal reflectance measurement is then taken in situ of each sample through the window of the chamber. It has been found that this method is highly reliable if samples (such as ZnO) are used that do not contaminate the window. The optical data are corrected for absorption and reflectance of the Suprasil window.

Irradiation of the samples is also performed through the window. A test is conducted by irradiating the samples for a period of time, interrupting the irradiation to make reflectance measurements, then resuming irradiation. This procedure is repeated until the desired amount of irradiation has taken place.

3.3 SPECTRAL PHOTOCONDUCTIVITY MEASUREMENTS

The spectral photoconductivity data presented are not intended to be a definitive study, but instead form a preliminary test to discover what general effects could be observed on sintered powders. A schematic of the laboratory set-up is presented in Fig. 9. The sample is placed in a vacuum bell jar and measured both at atmospheric pressure and high vacuum. Pressures attained are typically 10^{-6} Torr, using a liquid nitrogen trapped diffusion pump. Electrical measurements on the sample are made inside the

17

High vacuum valve

Roughing valve

Ion pump

Head with 4 sample positions

Fig. 8 Normal Reflectance U-V Irradiation Device

LOCKHEED PALO ALTO RESEARCH LABORATORY
LOCKHEED MISSILES & SPACE COMPANY
A GROUP DIVISION OF LOCKHEED AIRCRAFT CORPORATION

Electronics for measuring
conduction 4-point probe

Sample

4-point probe

Vacuum bell jar
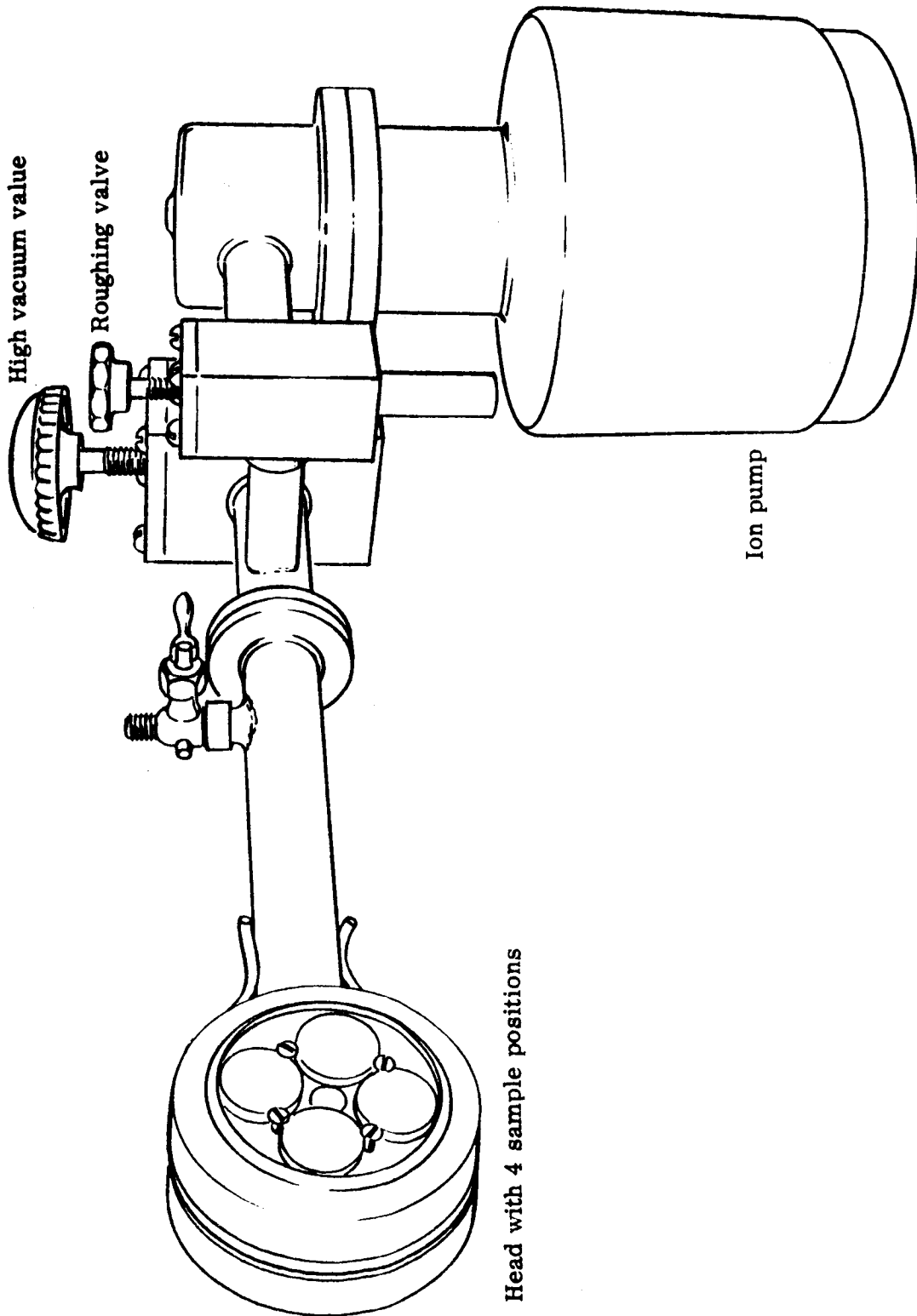
Monochromator

Tungsten light source
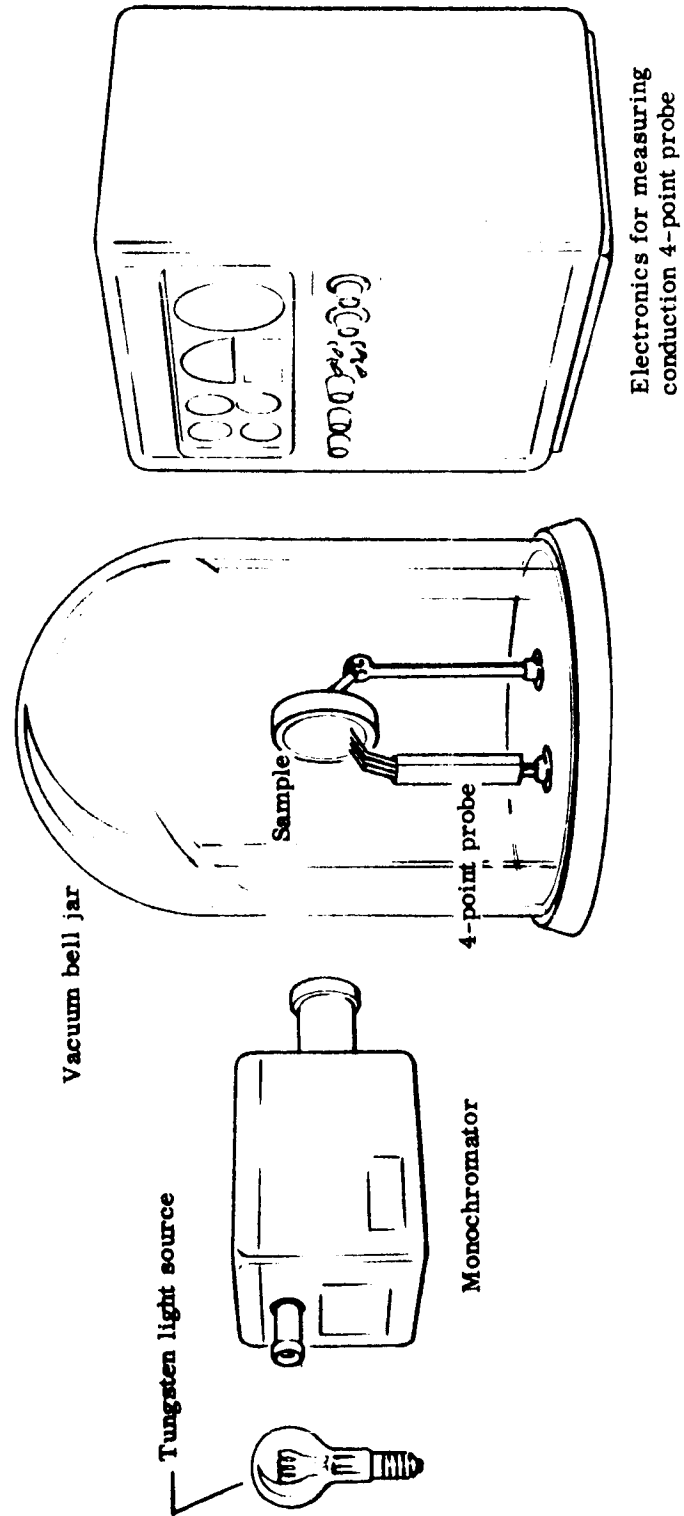
Fig. 9 Spectral Photoconductivity Apparatus

19

chamber with a 4-point probe, while the sample is irradiated monochromatically from outside the chamber through the Pyrex bell jar.

The uncertainty in the data arises from the fact that no attempt has been made to keep intensity constant as wavelength is varied. The intensity of the tungsten radiation source varies orders of magnitude within the spectral region studied. Therefore changes of slope, or the shape of a curve should be approximately correct, but comparison of magnitude throughout the spectral region cannot be made.

3.4 ELECTRON SPIN RESONANCE APPARATUS

The ESR apparatus is used to detect the gyromagnetic ratio of an unpaired electron by inducing transitions between the electron Zeeman levels, detecting these transitions and visually displaying them. The detection of these transitions is not a difficult task and there are many ways of doing it. For this purpose, the Varian 4500 EPR spectrometer was employed. This apparatus uses an impedance bridge system where the oscillator is isolated from the load. Figure 10 is a block diagram of this reflection-type microwave impedance bridge system which employs a crystal detector. Since the free electron precessional frequency is 2.8026 Mc/G, it is convenient to use x-band microwave equipment $(8,000-12,000$ Mc/sec) with an applied magnetic field in the region of 3000 G.

The source of microwave power is a klystron which delivers $1-2$ mW to the cavity. Using 100 kc/sec magnetic field modulation one can detect 3×10^{-13} ΔH moles of electron spins where ΔH is the line width of the signal expressed in gauss. This number is equivalent to 10^{-11} moles of dpph which was used as a standard for measuring the g-values.

For room temperature studies the source noise is the limiting factor for the signal-to-noise ratio. For this reason, the ZnO studies were performed at 79°K.
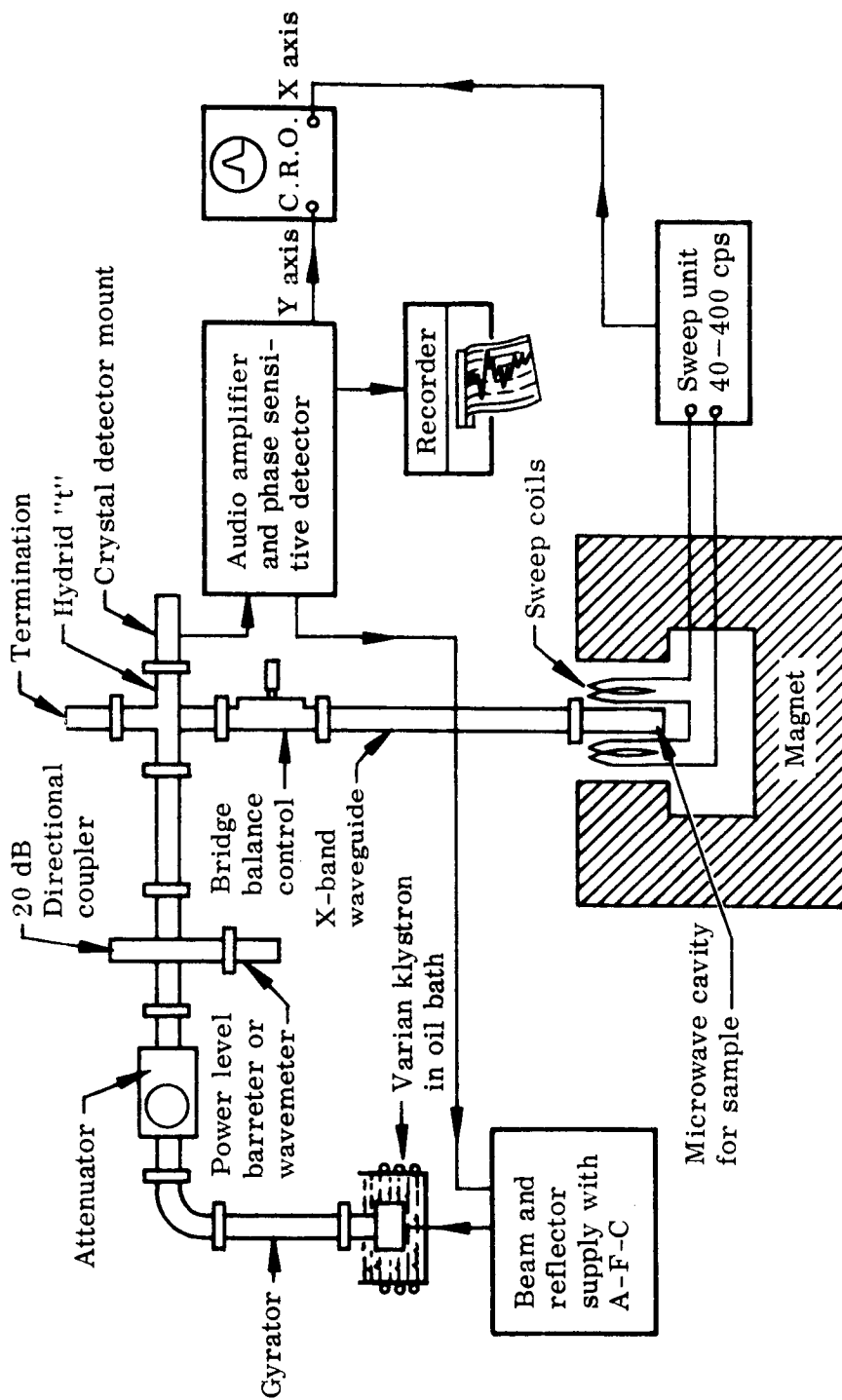
Fig. 10 Block Diagram of X-Band EPR Spectrometer

3.4.1 Sample Preparation and Treatment

The ZnO samples were prepared from SP-500 ZnO powder supplied by the New Jersey Zinc Corp. The powder was pressed at 600 psi into wafers (3 mm thick and 2.5 cm in diameter) and sintered in air at 600°C for 30 min. The wafers were broken into small fragments and shaped into cylindrical solid pieces ($\sim$ 6 mm long and 1.5 mm in diameter) with a surgical knife. Each sample was carefully weighed and placed into a standard Varian quartz sample tube (25 cm long and 4.75 mm in diameter). The sample tube was then mounted on the end of a flexible vacuum line which afforded complete freedom to move the sample into and out of the ESR cavity without disturbing the vacuum. A portion of the quartz Dewar above the cavity was unsilvered to permit radiation from the outside to reach the sample.

3.4.2 U-V Lamp and Accessories

The source of radiation consisted of a PEK A-H6 lamp housed in a water-cooled jacket made of quartz. The total irradiance at the sample during irradiation was 225 mW/cm^2 which is equivalent to 6.5 U-V suns based on 36% of the total energy content of the lamp spectrum in the range 2000−4000 Å.

Initially the sample was cooled by a stream of liquid nitrogen during irradiation. Immediately after irradiation, the sample was placed in the cavity for measurement; the flexible vacuum line allowed the vacuum to be maintained during the transfer of the sample. However, this method was not adequate since ice easily formed around the sample tube and reduced the incident radiation reaching the sample. The method finally adopted consisted of irradiating the sample in a bath of liquid nitrogen. The sample tube was raised just out of the cavity but remained in a quartz Dewar containing liquid nitrogen. The U-V radiation passed through the Dewar and liquid nitrogen to the sample. After irradiation the sample was merely lowered into the cavity with minimal mechanical and thermal disturbances.

3.4.3 Procedure

The sample was initially prepared and mounted in a quartz tube. In the presence of air at 760 Torr, the spectrum was observed. Then the sample tube was evacuated to 10^{-5} to 10^{-6} Torr and re-measured. Following this step, the sample was raised to the window level and irradiated for a time interval varying from 5 min to 2 hr depending on the particular sample being observed. After lowering the sample into the cavity, the spectrum was re-measured. It was discovered that the peak-to-peak height of the recorded first derivative curve decreased exponentially during the first 10 min following the radiation treatment. This is attributed to the change in electrical conductivity of ZnO induced by U-V irradiation which takes 10 min to decay to a minimum value. Since the altered electrical conductivity changed the Q of the cavity and affected the balance of the microwave bridge, the measurement was postponed at least 10 min following irradiation. This resulted in reproducible data and greatly improved the accuracy of the measurements. This procedure of irradiation and measurement was repeated at regular intervals. Other treatments include the addition of air at 760 Torr in the absence of U-V radiation, and re-irradiation of the ZnO in the presence of air at 760 Torr, and also at 10^{-5} to 10^{-6} Torr. For the most part, the measurements were performed at 79°K since the room temperature spectrum of ZnO was barely perceptible within the noise spectrum. It was also possible to irradiate the sample through slits in the end of the cavity without removing the sample.

3.4.4 Measurements and Reduction of Data

Intensity Versus Ruby. For each treatment of the sample, the peak-to-peak height and line width of the recorded first derivative curve were measured for ZnO and an intermediate standard − a ruby crystal mounted permanently within the cavity. Because the g-value of ruby is anisotropic, it was possible to orient the crystal so that the ZnO and ruby resonance lines were far apart.

The use of an intermediate standard permitted evaluation of the relative spin concentration of the two systems. The absolute spin concentration of ruby was obtained

by comparing ruby to a dilute solution of manganous sulfate of known concentration. This value (2.8×10^{18} spins) was then used to compute the absolute spin concentrations of the ZnO resonance line.

Calculation of g-Values. The g-values for the ZnO resonance lines were obtained by measuring the magnetic field displacements between the ZnO and dpph resonance lines. From the g-value used for dpph (2.0037) it was an easy matter to obtain the ZnO g-values.

Use of NMR for Measuring Magnetic Field. In order to measure the magnetic field, a NMR Precision Gaussmeter* was used in conjunction with a Hewlett-Packard 524B electronic counter (10−100 Mc). The gaussmeter is designed to provide extremely accurate and rapid measurements of constant or slowly changing magnetic field. As used here, the measurements were based on proton resonance and yielded 0.01% accuracy.

---

*Model G-501 Harvey-Wells Electronics, Inc.

Section 4
SAMPLE CHARACTERIZATION

Three types of samples were used on this program: high purity ZnO powder, S-13 paint, and ZnO single crystals. The reason for this variety of systems studied is that by looking at the material in its different forms, particularly in the powdered form and single crystal form, it is possible to distinguish between surface and bulk effects as well as between defect and intrinsic effects.

Powder. SP-500, produced by the New Jersey Zinc Co., was utilized for this phase of the program. SP-500 is 99.9% pure, and has an average particle diameter of 0.3μ. The powder is put in an easily studied form by pressing and sintering it into 2.2 cm diameter disks. The powder is pressed into a disk at 600 psi, and then sintered without pressure applied for 1/2 hr at 600°C in air. The resulting disk has excellent mechanical strength and thermal conductivity.

All tests in this program were conducted near room temperature, so it was possible to obtain good thermal contact between the sintered disk and the substrate by employing an epoxy adhesive. The adhesive is stable in high vacuum at room temperature, and does not affect the samples.

Paint. The paint used was S-13. prepared by the Illinois Institute of Technology Research Institute. This paint incorporates SP-500 ZnO pigment into a methyl silicone elastomer binder. It has been found that the U-V degradation characteristics of the paint are equivalent to those of the sintered pigment, as studied in the bidirectional reflectance equipment.

Single Crystal. The single crystal was obtained from Minnesota Mining and Manufacturing Co. It was sectioned into pieces a few millimeters thick and polished. The resulting crystal was about 1/2 cm in diameter and 1 mm thick.

25

The advantage of studying the single crystal in conjunction with the powders is that single crystals have fewer defects, and a measurement of their optical properties involves fewer surfaces. Most fine-particle-size powders, such as SP-500, are made in such a way as to incorporate an enormous amount of defects in the particles. These defects may take several forms, a few of which are vacancies, dislocations, twinning, and grain boundaries. By contrast, the single crystal is prepared very carefully, and grown slowly so that the defect level may be considered near a minimum. An optical measurement is made on a single crystal by shining light on it and measuring the portion transmitted. This involves only two surfaces. The powder, on the other hand, is measured optically by measuring the energy that is reflected by it. Before this energy may be reflected, it must have been transmitted through, reflected from, and scattered from many particles. Thus, measurements made on powders are more sensitive to surface properties than are single crystal measurements.

When a model is to be constructed, it is necessary to know where the damage centers are generated, where they reside, and whether they involve creation of defects or defects that were already present. Thus the contrast and comparisons between single crystals and powders, which represent two extremes in these respects, can be quite revealing.

26

Section 5
EXPERIMENTAL RESULTS

5.1 U-V DAMAGE TO ZnO ELECTRICAL AND OPTICAL PROPERTIES

5.1.1 Reflectance in the Visible and Near IR

When samples of sintered ZnO are exposed to U-V radiation in vacuum their reflectance decreases. Such decrease is shown in Fig. 11, for a sample irradiated at room temperature, 10^{-6} Torr pressure, and 5 suns intensity for 205 hr. A sun here is defined as that amount of energy flux in the solar spectrum from 0.2 to 0.4 μ per unit area at 1 AU. These conditions are typical for a U-V test, and these data will serve to represent the damage that is to be expected from this material when radiated with U-V energy. Data for Fig. 11 were obtained in two ways. Reflectance spectra of the material were taken at ambient conditions with the Cary Model 14 before and after exposure to the radiation. Reflectance spectra were taken in situ with the bidirectional reflectance device.

It may be seen immediately that there are two distinct spectral regions of damage, one in the visible, and one in the infrared. It will be of interest throughout this report to study the kinetics of damage to each spectral region. A convenient way of doing this is to plot the reflectance at a representative wavelength for each spectral region versus time. Alternatively, change in reflectance may be graphed as a function of time. Both methods have been utilized in this report.

The two spectral regions of damage are different in nearly every respect that has been tested. Two differences may be seen in Fig. 11. First, the decrease in reflectance in the IR is more severe than in the visible. Second, the damage to the IR recovers completely upon admission of oxygen to the chamber, while the damage to the visible does not.

27

205 hr Total irradiation time
Room temperature
$P \cong 10^{-6}$ **Torr**
TP 18459

———— Initial normal reflectance in air
·—·—· Final normal reflectance in air
- - - - - Final bidirectional reflectance <u>in situ</u>
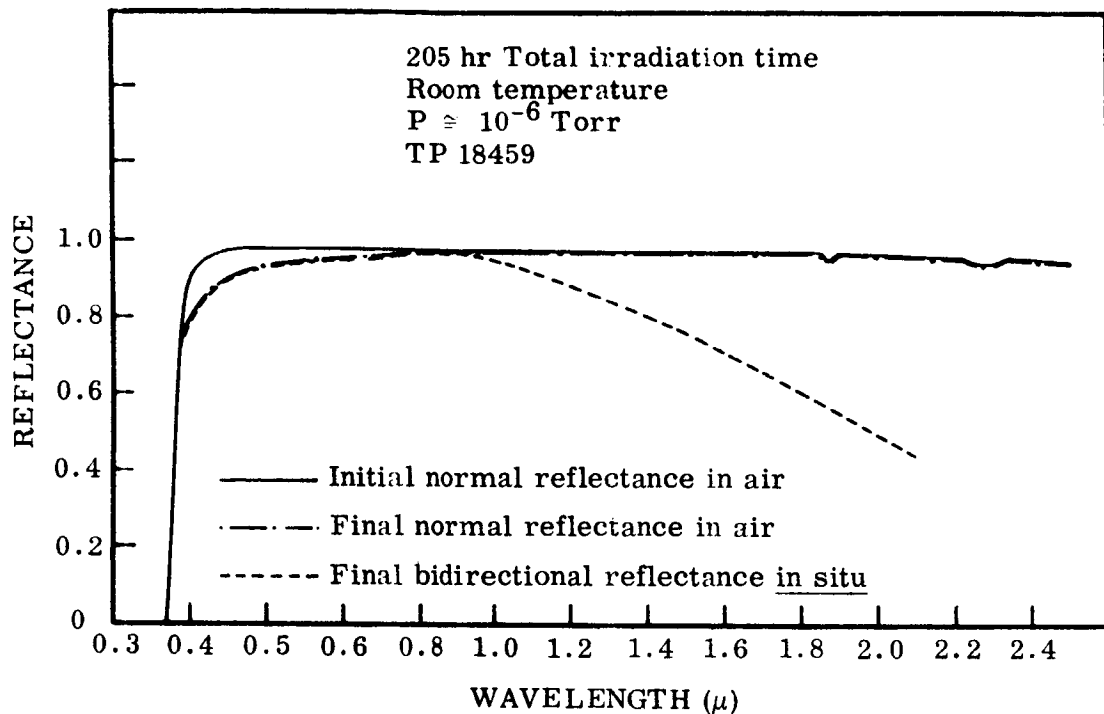
Fig. 11 Reflectance History of SP-500 Under 5 suns U-V Irradiation

Several conclusions may be drawn from these initial observations. First, the states causing the I-R absorption must reside on the surface of particles. This is required for the rapid recovery upon admission of oxygen to take place. Second, the damage to the visible must either reside in the bulk, or be relatively insensitive to the presence of oxygen if it is on the surface. Third, the I-R damage centers must be directly associated with oxygen, for the recovery in pure oxygen to have occurred.

5.1.2 Temperature Effects

The effect of temperature on the reflectance in each of the spectral regions was established in earlier work (Ref. 15). The results are stated here for completeness.

The reflectance in the visible region decreases, typically, 0.05 at room temperature. At about 100°C the visible decreases ~ 0.10 to 0.15; 0.30 to 0.40 is a typical drop for

28

about 200°C, and for temperatures any higher than this free zinc is given off by the sample so profusely that the measurement equipment is contaminated and measurements become impossible.

The I-R changes with temperature of irradiation are less drastic. There may be a difference of as much as a factor of 2 in reflectance between liquid nitrogen temperature and 200°C, but nothing so dramatic as the factor of 10 that occurs for the visible region.

The effect of temperature variation, then, is to increase the damage in each of the two spectral regions, but no new absorptions appear.

The principal result of this phase of the study is the strong temperature dependence of the damage in the visible. It must be concluded that the damage in this region involves mass transport in the bulk of the particle; i.e., diffusion.

The weaker temperature dependence of the I-R damage may be due to surface diffusion or desorption since it has already been established that the damage centers in this case reside on the surface.

5.1.3 Resistance Changes During Irradiation

The resistance of the sintered samples has been measured throughout several U-V tests, and the results correlated with the optical damage to gain further insight into the cause of the optical damage. The difficulties of this measurement prevent precise correlation. Electrical measurements on powders are complicated immensely by inter-particle effects. There are potential barriers between particles, and necks connecting them both inhibiting the ohmic behavior of the intrinsic material. Thus changes in the intrinsic particles may be masked by changes in the inter-particle properties.

Figure 12 shows I-R reflectance and resistivity as a function of time during irradiation. The curves are deceptively symmetrical. Subsequent tests have shown that the changes in slope of the two curves do not, in general occur at precisely the same time as they do in Fig. 12. The one conclusion that can be made for all the conductivity data that have been taken (but not included here because it would be repetitive) is that when reflectance in the IR goes down, so does resistance. Thus it is evident that there is a relationship between the I-R reflectance and electrical conductivity.
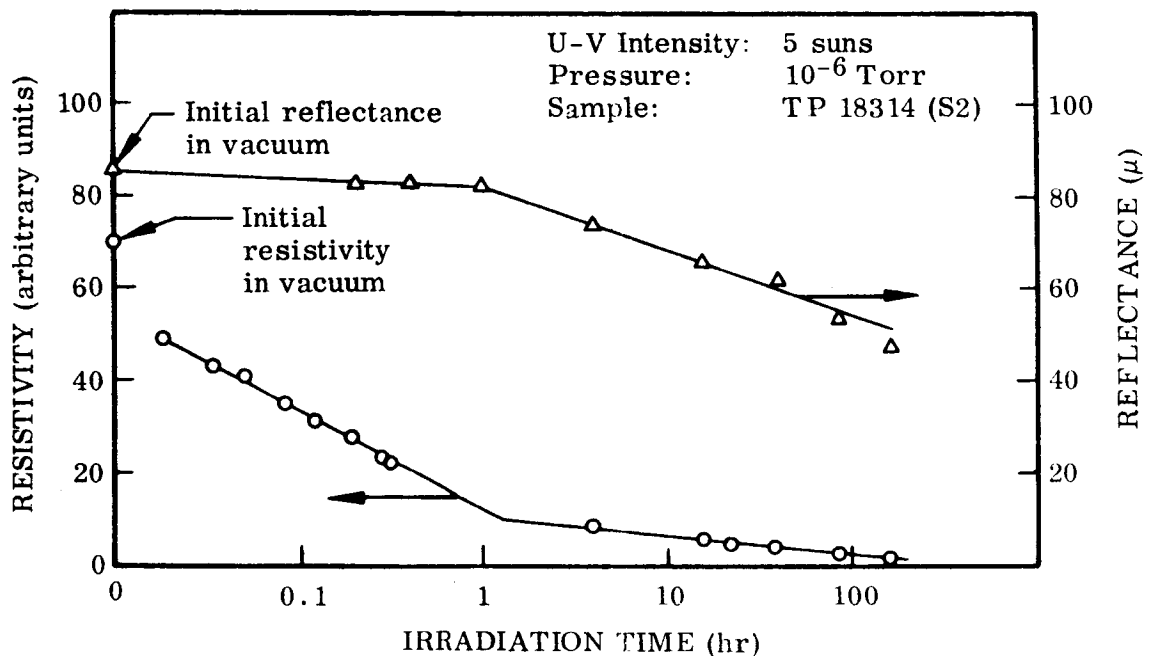
Fig. 12 Simultaneous U-V Damage and Conductivity Measurements on ZnO in Situ

5.2 RECOVERY OF U-V INDUCED DAMAGE

As has already been stated the damage to sintered samples recovers upon admission of oxygen to the chamber after U-V degradation has taken place. Figure 13 shows the change in reflectance in the two damage regions when oxygen is admitted at two different pressures, and with and without irradiation. It may be seen (1) that there is no

30
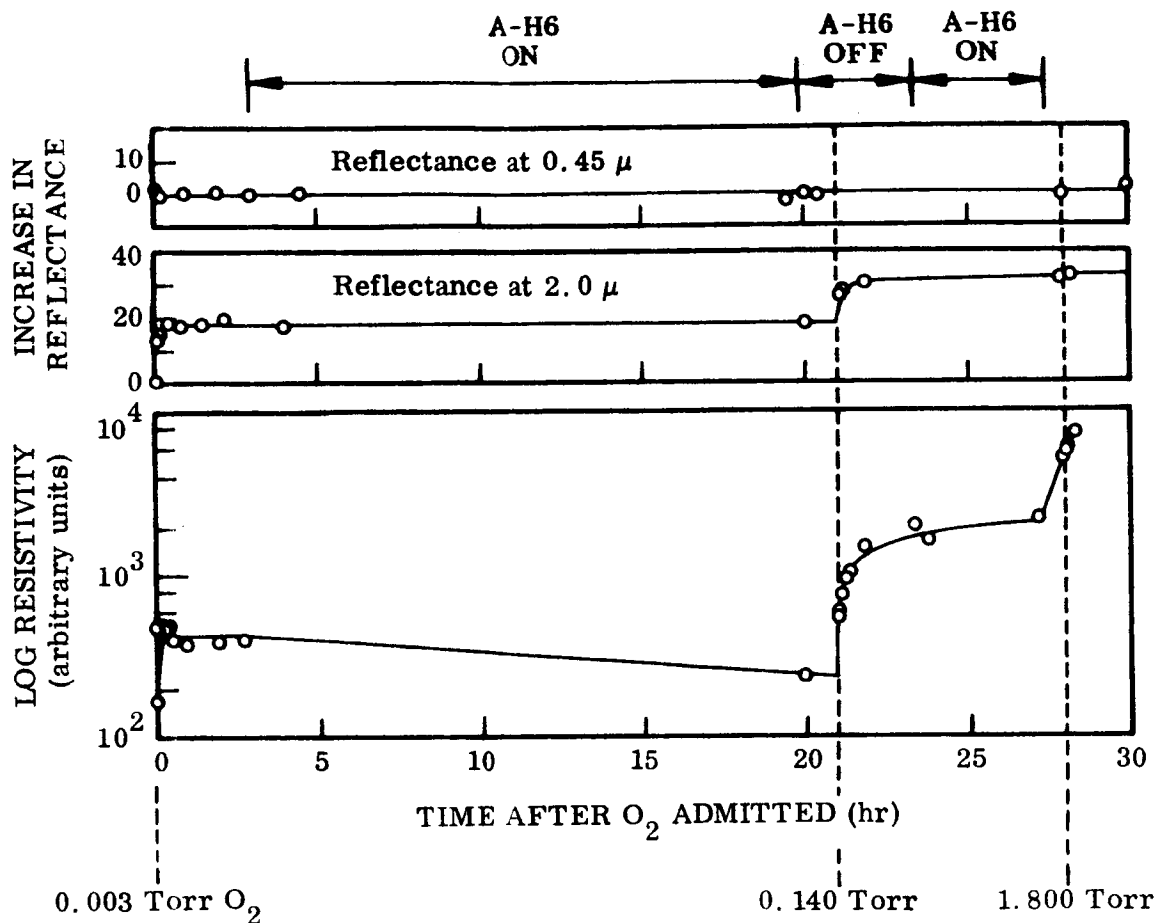
Fig. 13 Reflectance and Resistivity of ZnO During Recovery Under Irradiation

effect of the radiation, (2) that the visible region does not recover substantially, (3) that the IR recovers rapidly, and (4) that the I-R reflectance reaches an equilibrium value of reflectance dependent upon the partial pressure of oxygen.

The effect of pressure of oxygen on the rate of recovery is shown in Fig. 14 in more detail. Two samples with different irradiation histories, and thus different total amounts of damage, are recovered at pressures differing by two orders of magnitude. Yet it is seen that the initial rates of recovery are quite similar. The major difference between the two curves appears to be the extent of final recovery — the lower pressure producing less recovery. The influence of oxygen pressure rather than extent of

31
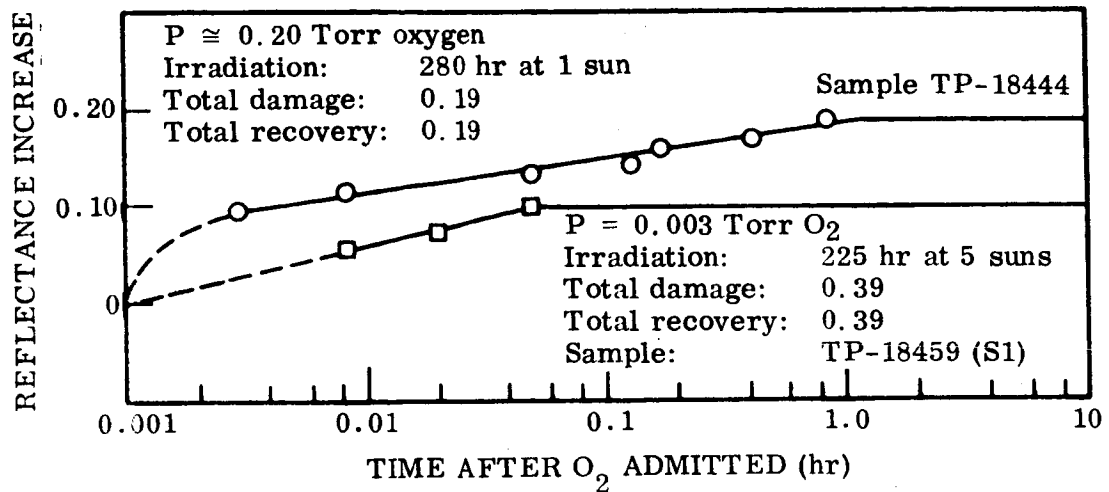
Fig. 14   Recovery of Sintered ZnO at Two Pressures After Different
Irradiation Histories

damage is indicated by the fact that the more heavily damaged sample exhibited less recovery.

In recovery, as in damage, the general trends of the I-R reflectance coincide with those of the sample resistance, but the details do not. Figure 13 compares resistance and reflectance during recovery at several pressures and with and without irradiation. When the pressure in the chamber was 0.003 Torr, the resistance dropped under the effect of the UV, but the reflectance at 2.0 μ did not. Further, when the pressure in the chamber was 1.8 Torr, and the UV was extinguished, the resistance increased, but the reflectance did not.

Further discrepancies between optical data and electrical data may be seen in Figs. 15 and 16. In addition, discrepancies may be observed between electrical data from one sample to the next, despite the samples being exposed simultaneously to identical conditions. It may be seen that the reflectance recovery curve and the optical recovery curves do not have the same shape for either case. Further, the recovery curves for the electrical properties of the two samples are not similar.

32

Fig. 15 Recovery of Optical and Electrical Properties of Sintered ZnO

Fig. 16 Recovery of Optical and Electrical Properties of Sintered ZnO

33

LOCKHEED PALO ALTO RESEARCH LABORATORY

L O C K H E E D   M I S S I L E S   &   S P A C E   C O M P A N Y
A   G R O U P   D I V I S I O N   O F   L O C K H E E D   A I R C R A F T   C O R P O R A T I O N
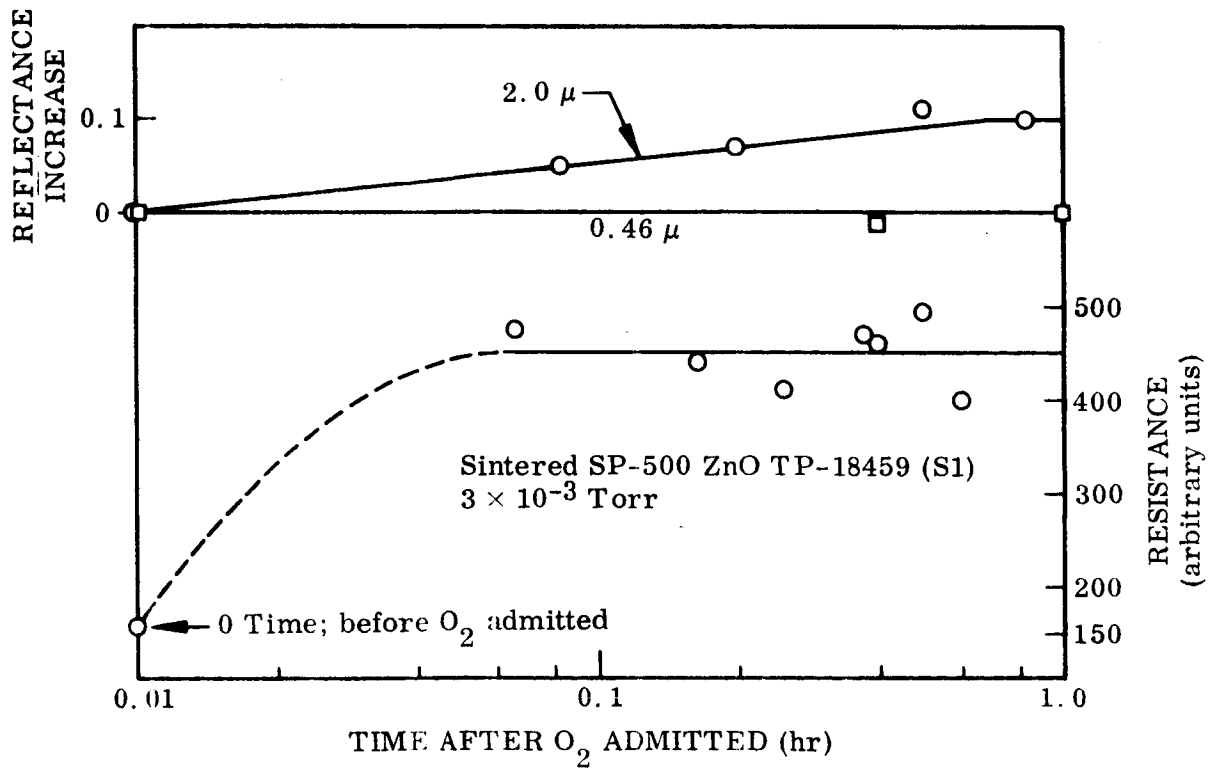
The conclusions of this section are as follows:

- The visible reflectance does not recover immediately upon admission of oxygen to the chamber, but exhibits partial recovery over a period of many days.
- The near I-R reflectance does recover rapidly upon admission of oxygen to the chamber.
- The resistance of the samples recovers upon admission of oxygen to the chamber.
- Radiation does not affect the recovery of optical properties.
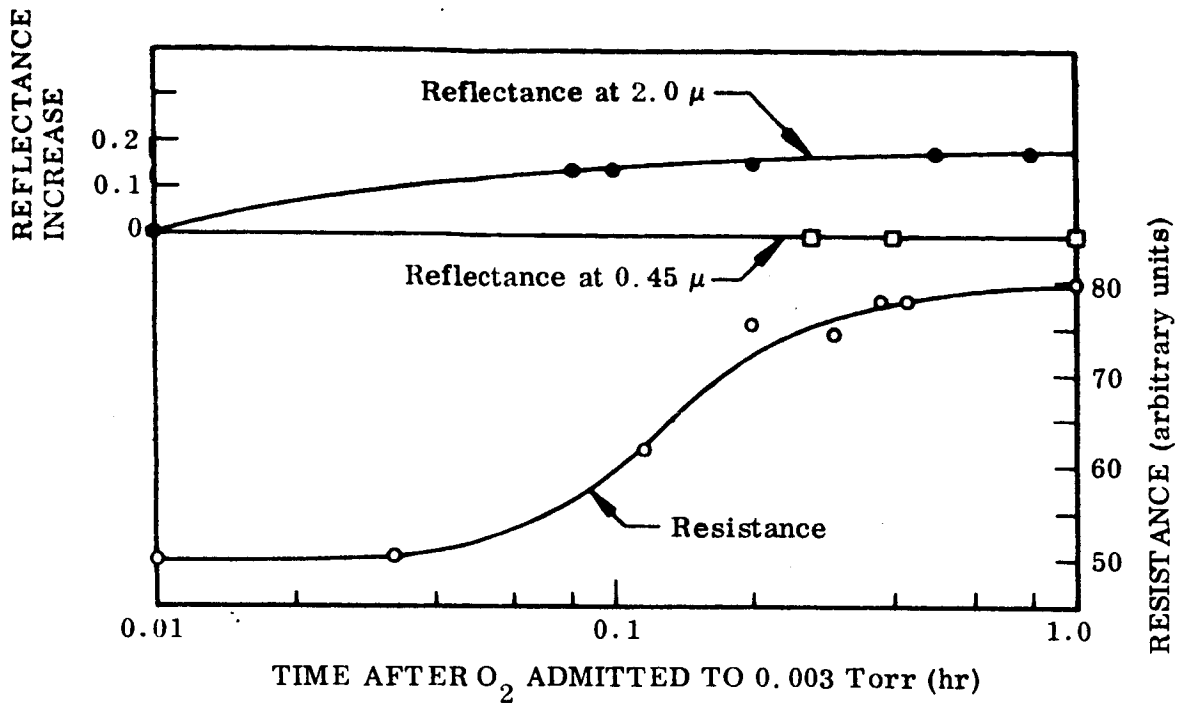- Electrical properties and the reflectance of the IR are related but the details are not fully understood.

5.3 SELECTIVE WAVELENGTH IRRADIATION OF PARTICULATE ZnO

The U-V irradiation of ZnO in vacuum produces reflectance degradation in two distinct wavelength regions, the U-V and visible regions adjacent to the band edge and the I-R region between 0.8 and 2.7 μ. It is essential to the understanding of the degradation to determine the photon energy required to produce absorption in each spectral region and to determine if the two regions of degradation are related or independent of each other. For this purpose several experiments involving selective wavelength irradiation of ZnO were performed.

The photoresponse is a maximum at the band edge because there the absorption coefficient is large enough to produce photocarriers but small enough ($\alpha \sim 10$ cm^{-1} at 0.39 μ, Ref. 20) that the radiation penetrates deeply into the sintered sample. For shorter wavelengths the absorption is much stronger ($\alpha \sim 10^5$ cm^{-1} at 36 μ, Ref. 20) causing significant photocarrier production in the surface layer of particles, but beneath the surface layer only a few particles are irradiated. For longer wavelengths, the irradiation penetrates deeply into the sample, but the absorption is very weak. Nevertheless photoresponse does occur for wavelengths as long as 0.60 μ. All evidence (Refs. 21−23) indicates that photoconductivity is due to desorption of

34

chemisorbed and possibly lattice oxygen with accompanying injection of carriers into the conduction band. If the diagnosis of photoconductivity is correct, it should be possible to cause significant photodesorption of oxygen with photons less energetic than the band gap of 3.2 eV and possibly also produce optical absorptions in the near IR. The I-R absorption might be due either to absorption by the increased number of free carriers accompanying photoconductivity or to defects resulting from lattice photolysis by the less-than-band-gap photon energies.

5.3.1 Spectral Photoconductivity of Sintered ZnO

The steady-state slow photoconductive response of a standard sintered sample was determined in air and vacuum. The sample was irradiated monochromatically with a tungsten lamp source as described in Sec. 3.3. The results are presented in Fig. 17. The photoconductive response has not been corrected for sample geometry and for spectral radiance of the tungsten lamp which varies significantly in the visible and near U-V spectrum.
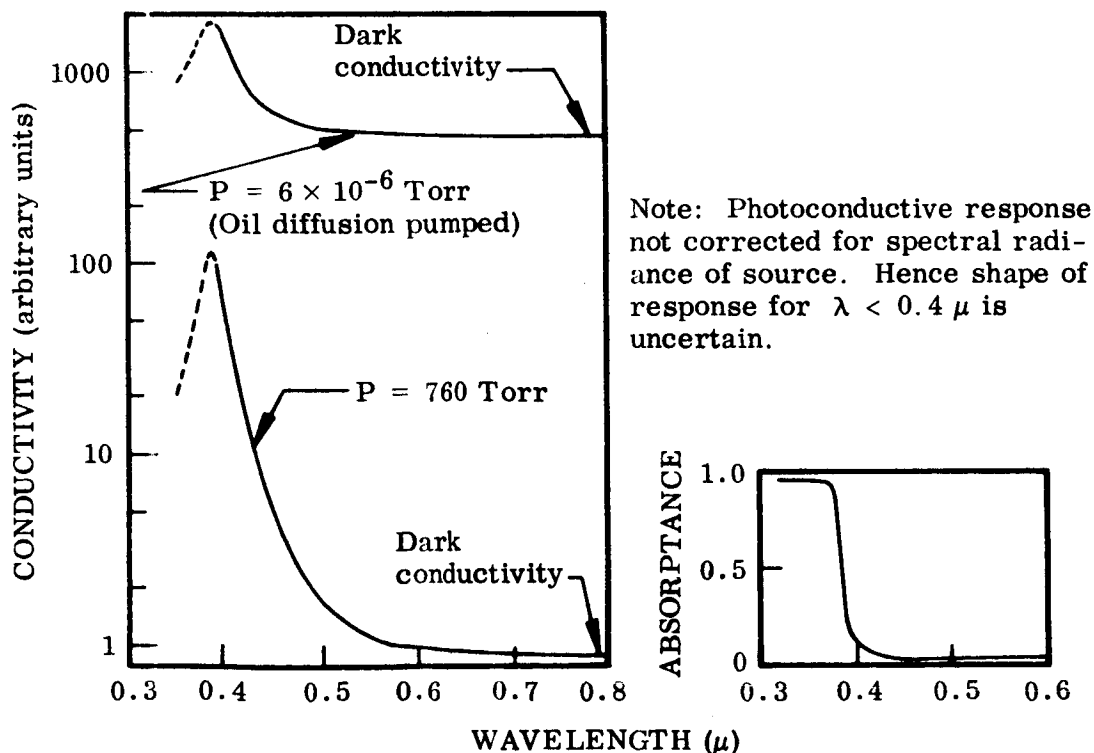

Note: Photoconductive response not corrected for spectral radiance of source. Hence shape of response for $\lambda < 0.4 \, \mu$ is uncertain.

Fig. 17 Spectral Photoconductivity and Absorptance of Sintered ZnO

35

Without correction for irradiation flux it cannot be determined whether the photo-response decreases or remains nominally constant for $\lambda < 0.38\,\mu$, but this is not of great importance. The significant data given in Fig. 17 are as follows: (1) there is a peak response near the band edge; (2) there is a photoresponse for $\lambda \leq 0.60\,\mu$; and (3) there is a large increase in dark conductivity due to vacuum.

5.3.2 Spectral Irradiation of Sintered ZnO and S-13 Coating

To explore the above possibility, a series of filtered irradiation tests were conducted on sintered ZnO. An A-H6 source was used at a lamp-to-sample distance that would correspond to 10 suns if no filters protected the samples. Two sintered samples were irradiated with selected wide band-pass filters interposed between source and samples in the apparatus described in Sec. 3.2. This apparatus is operated so that no start-up glow discharge occurs during pump-down. The importance of this detail is explained in Sec. 5.4. The transmission characteristics of the filters are shown in Fig. 18. The U-V radiation did not affect filter transmission. The kinetics of reflectance degradation in the visible (represented by $0.45\,\mu$) and in the infrared (represented by $2.0\,\mu$) are shown for each sample individually in Figs. 19 and 20.

It is seen that no absorption in the IR or visible occurs due to 130 hr in vacuum and dark. Hence the increase in dark conductivity observed in Fig. 17 does not coincide with increased I-R absorption. This indicates that chemisorbed oxygen is lost in the dark, in vacuum due to thermal activation, but the released free carriers do not pro-duce measurable absorption.

When a sample is irradiated with wavelengths longer than $0.65\,\mu$, no I-R absorption results (Fig. 20). This is consistent with the absence of photoresponse for $\lambda > 0.6\,\mu$. When the photon energy is increased by using 3-70, 3-71 and 3-72 filters there results a small degradation in I-R reflectance. In Fig. 19, a significant photoconductive response is observed for wavelengths passed by these filters. When the 3-75 filter is used, the I-R absorption increases markedly which is consistent with the large photoresponse for wavelengths near $0.39\,\mu$.

36
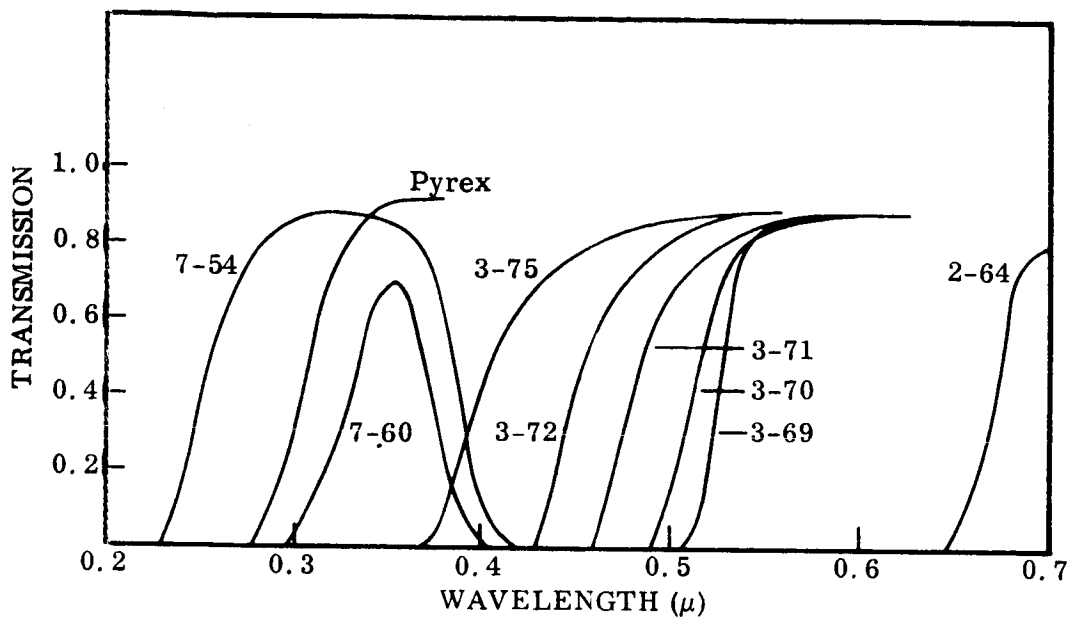
Fig. 18 Transmission of Filters Used in Irradiation of ZnO
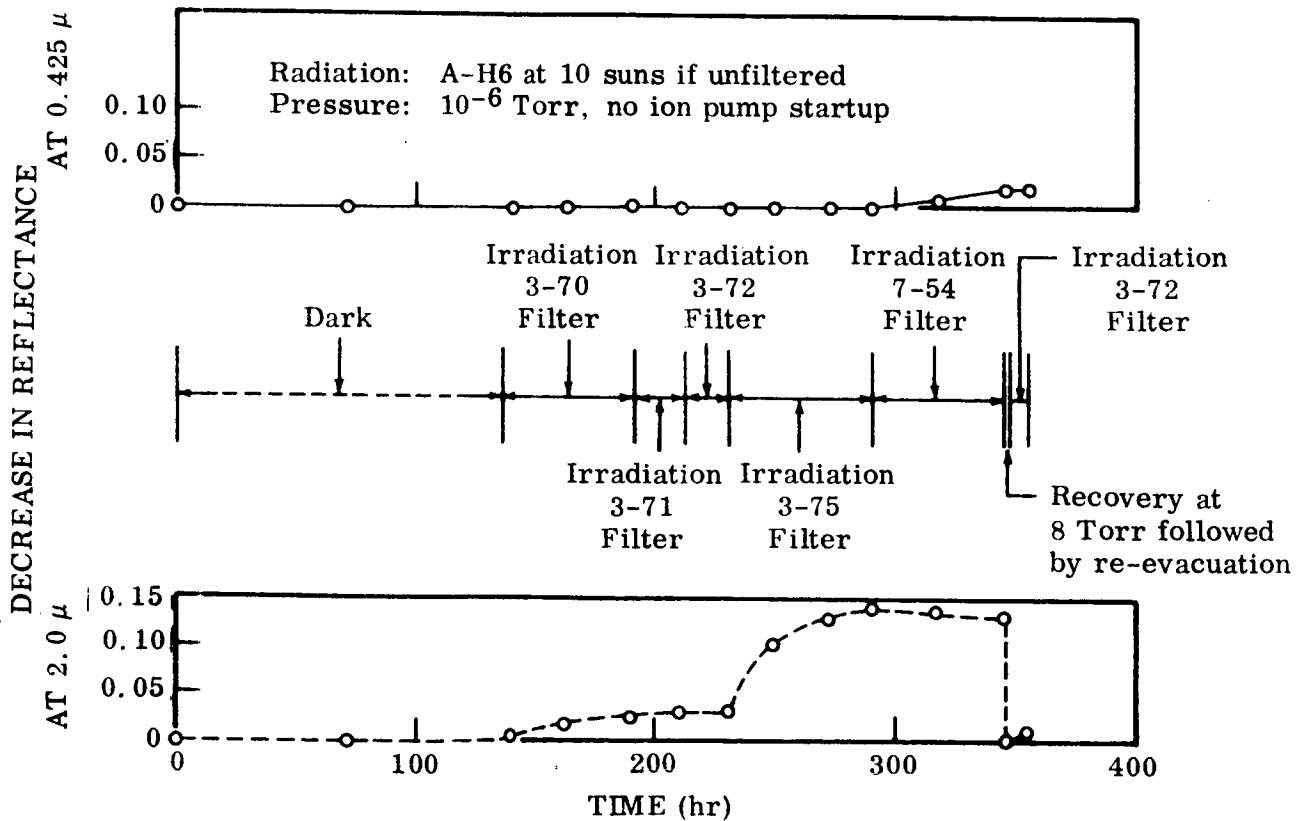
Fig. 19 Effect of Spectral Irradiation on Reflectance of Sintered ZnO

37
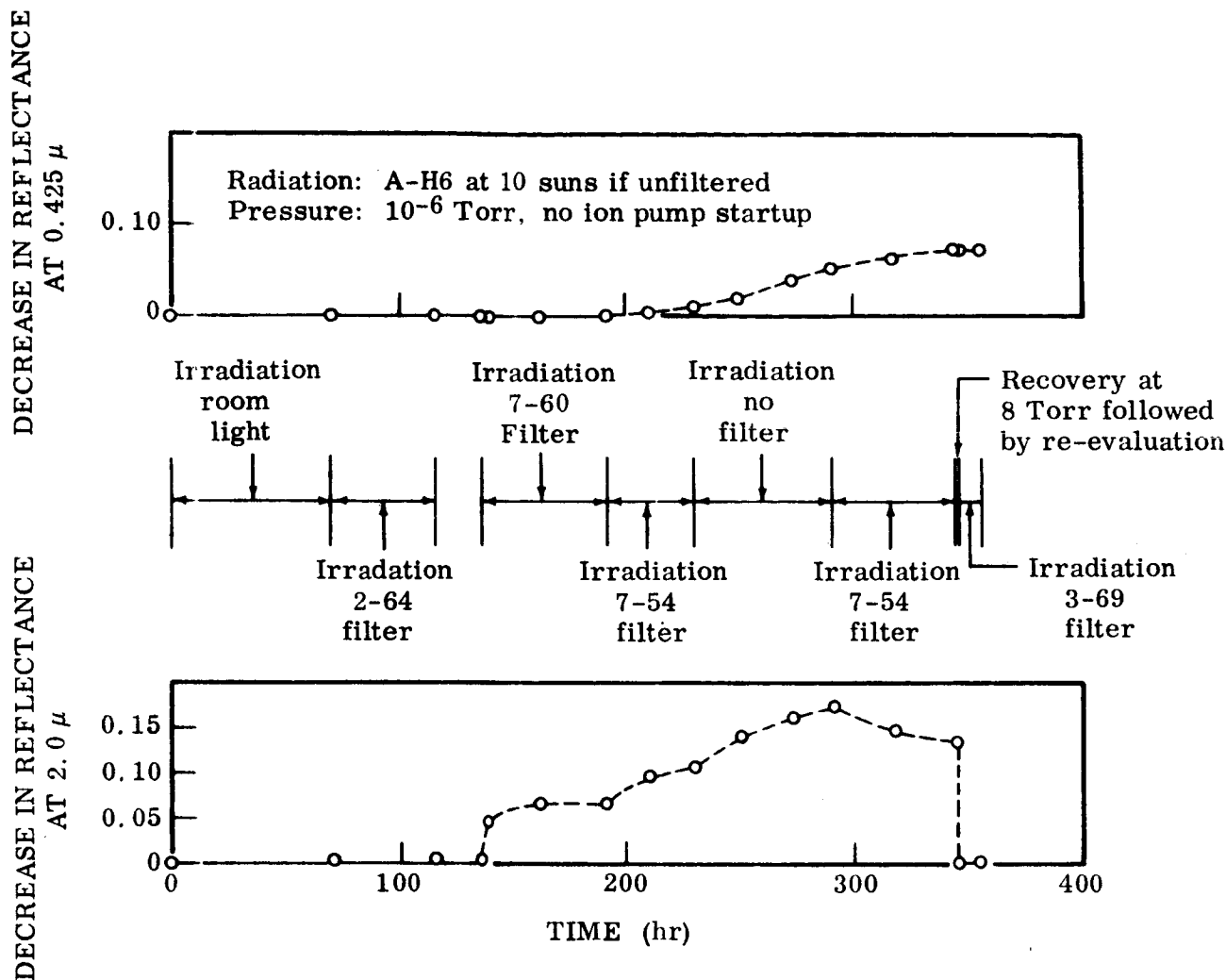
Fig. 20 Effect of Spectral Irradiation on Reflectance of Sintered ZnO

Upon comparison of the I-R degradation due to wavelengths longer than 0.38μ with that due to U-V wavelengths transmitted by the 7-60 and 7-54 filters (Fig. 20) it is apparent that the I-R degradation is produced most effectively by wavelengths near 0.39μ. The photoresponse shows that these wavelengths are absorbed, but the absorption constant for $\lambda > 0.39 \mu$ is less than 10 cm^{-1}. Therefore photons of wavelengths longer than 0.39μ are scattered through many particles deep below the sample surface, and cause photodesorption from a large total particle surface area. Since the IR is apparently absorbed only weakly by the resultant defects, a large population of defects must be produced to cause significant I-R absorption. It follows then that even though energetic UV may have a higher quantum yield for photodesorption of oxygen, its effects are

38

confined to the first few layers of particles because it is strongly absorbed ($\alpha = 10^5 \, cm^{-1}$ for $\lambda < 0.36 \, \mu$). Hence the total surface area affected is small, and little I-R absorption results.

Additional evidence that wavelengths longer than $0.38 \, \mu$ are the principal cause of I-R degradation in particulate ZnO is given in Fig. 21 for S-13 coating. It is shown that the sample protected by Pyrex degrades in the IR at the same rate as that exposed to the entire A-H6 spectrum.
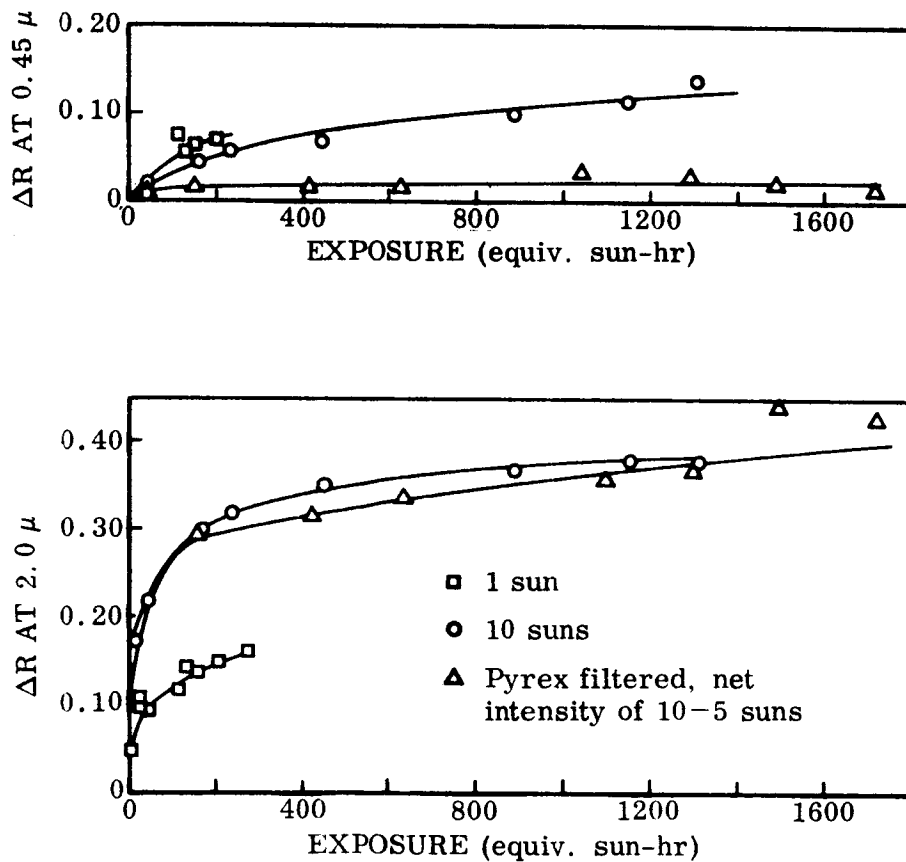
Fig. 21   Change in Reflectance of S-13 at 2 and $0.45 \, \mu$ for Irradiation at 1 and 10 suns Intensity

39

The evidence thus far on spectral irradiation indicates that at least two species of oxygen-related states are involved in ZnO photoelectronic properties. The first species which can be desorbed in vacuum and dark increases the conductivity but produces no optical absorption. The second species must be photodesorbed to produce optical absorption in the IR. The second species also contributes to particle conductivity.

Another important consideration is the relationship between I-R and visible absorption caused by irradiation. It was postulated in earlier work (Ref. 15) that I-R absorption caused by oxygen photodesorption resulted in excess zinc at the particle surface which could diffuse interstitially and produce the visible absorption. If this general model is correct, it would help to know if the second event necessarily follows from the first. The data on spectral irradiation answer this question. It is clear in Fig. 21 for S-13 that even though two samples incurred equivalent I-R degradation the Pyrex filtered sample exhibited much less visible absorption. Hence it appears that U-V radiation of wavelengths $0.2 < \lambda < 0.3$ is necessary to produce significant visible absorption. The same conclusion is reached by comparing the visible degradation resulting with a 3-75 filter and no filter in Figs. 19 and 20. With equivalent I-R damage, the photons transmitted by the 3-75 filter produce no visible degradation. It is interesting to note that the visible degradation can occur subsequent to, rather than simultaneously with I-R degradation. Once I-R degradation is produced, Figs. 19 and 20 show that visible degradation proceeds with U-V irradiation transmitted by a 7-54 filter even though the I-R absorption is diminishing.

Significant information could be gained if it could be established whether visible degradation can be produced in particulate samples without I-R degradation by irradiation. If it is possible this would require a revision of the degradation model which postulates a causal connection between I-R and visible absorption. The attempt to provide this information incorporated filters which transmit UV only and thereby minimize the I-R degradation. The results were not conclusive because significant I-R degradation was produced. Hence this question remains to be answered.

40

It can be concluded from the spectral irradiation tests that (1) the I-R absorption is produced most efficiently in zinc oxide powders by photons slightly less energetic than the band-edge at 3.2 eV and (2) energetic U-V photons, 4 to 6 eV are required for effective production of visible absorption.

5.3.3 "Memory" of U-V Irradiated ZnO

It has been reported (Ref. 24) that after recovery from U-V degradation in air, ZnO powder exhibits a memory by redamaging in the IR due to vacuum only. To check this effect, two damaged samples were fully recovered at an air pressure of 8 Torr and then the chamber was re-evacuated to 10^{-6} Torr. No decrease in the I-R reflectance was observed due to re-evacuation. Following this the two samples were irradiated for 10 hr at 10 suns through 3-72 and 3-69 filters. Only very slight I-R degradation was observed for the sample irradiated through the 3-72 filter (Fig. 19). These results indicate that the recovered material has a surface configuration which is as stable as the original unirradiated sintered material. The apparent memory effect may perhaps be explained in terms of ion pump interactions with the samples as will be described in Sec. 5.4.

5.4 DEGRADATION OF SINTERED ZnO BY ELECTRONIC VACUUM PUMP

With one exception, all tests in this study with in situ optical measurements have been conducted in a vacuum chamber which is evacuated with a sorption roughing pump and electronic high vacuum (VacIon) pump. With the advent of simultaneous electrical conductivity measurements on sintered samples it was found that the sample conductivity increased approximately three orders of magnitude during ion pump start-up. It was clear that the conductivity increase was not due to a pressure change because the pressure remains nominally constant during the early periods of pump operation. The observed increase in conductivity led to subsequent discovery of an accompanying large decrease in I-R reflectance. Prior to the incorporation of conductivity measurements, it had been observed on occasion that the I-R reflectance decreased between

41

the initial <u>in situ</u> reflectance measurements in partial vacuum and measurements in high vacuum prior to ignition of the U-V source. It was assumed that this small decrease in reflectance ($R \approx 0.05$ at $2.0\ \mu$) was due to oxygen desorption in high vacuum. Now more detailed measurements have revealed that in all cases the ion pump start-up causes an immediate effect on the I-R reflectance of sintered ZnO. A representative history is shown in Fig. 22. It is apparent that the initial large degradation recovers over several hours so that the final net reflectance decrease is 0.05 to 0.10 in agreement with the earlier more superficial observations. In some earlier observations (Ref. 15), the decrease in I-R reflectance is substantially smaller than 0.05 to 0.10 at $2.0\ \mu$ indicating that the magnitude of the effect may vary considerably depending on the ion pump used. There is no simultaneous effect on the visible reflectance as represented by the wavelength $0.45\ \mu$ in Fig. 22. On S-13, the only coating tested, results indicate that there is no significant effect on the reflectance in the visible or IR probably because of a rapid charge accumulation on the silicone surface which repels further ion bombardment. However, work done on the
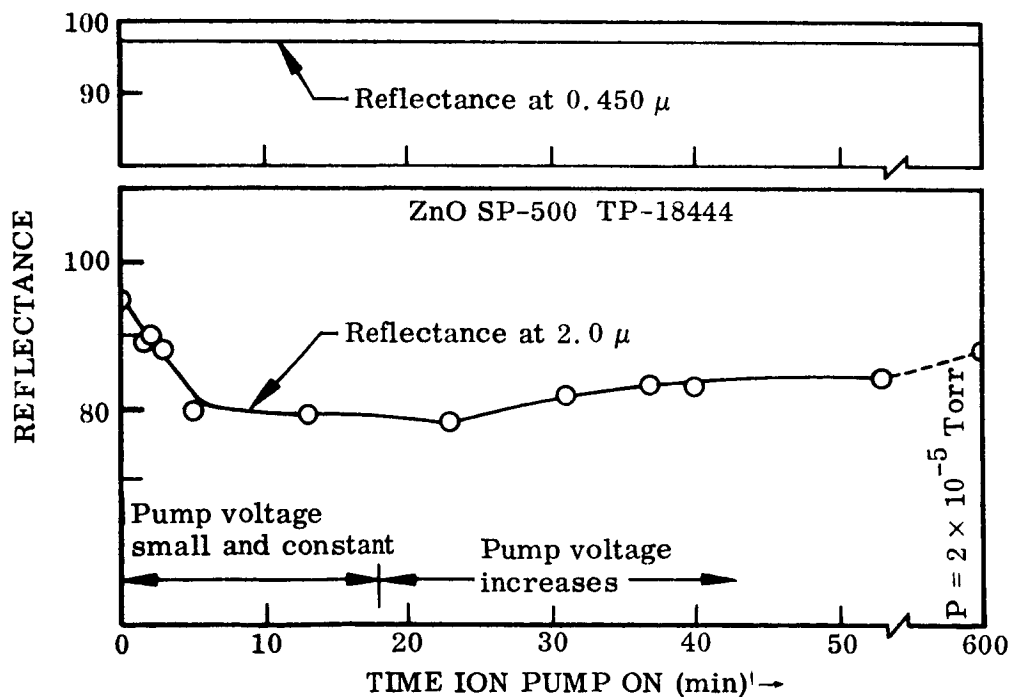

Fig. 22 Change in Reflectance Due to Ion Pump Start-Up

42

electrofax process and on solar proton degradation has shown that for more energetic ion fluxes, the properties of ZnO in an elastomer matrix can be substantially affected.

The samples are optically shielded from the active region of the pump by a number of metallic surfaces so it is evident that ions and not U-V photons from the start-up glow discharge are the cause of optical degradation. Efforts to eliminate the problem by placing various combinations of positively and negatively biased grids ($\pm$ 200 Vdc) in the ion pump throat to prohibit ion migration to the sample region were only partially successful. The grids reduced the ion and electron currents from approximately 20×10^{-9} to 1×10^{-9} A as measured on biased probes adjacent to sample positions. The effect of pump start-up on reflectance was only halved. Therefore, under the least severe conditions the reflectance of each sintered sample is briefly degraded about 0.10 at 2.0 μ followed by partial recovery and the conductivity is increased approximately three orders of magnitude prior to U-V irradiation.

There is serious question regarding the interpretation of the effects of the ion pump start-up on subsequent U-V degradation and recovery. The answers to this question are not fully in hand at this time, but a number of observations can be made. It was observed in the photoconductivity measurements in sintered ZnO (Fig. 17) that the dark conductivity increased about three orders of magnitude due to vacuum only (diffusion-pumped). Therefore the conductivity change produced by the ion pump is not alarmingly large. However, it was observed in a test reported in Figs. 19 and 20 that there is no change in I-R reflectance due to vacuum for periods of over 100 hr, if no ion pump is used. The effect of the ion bombardment on reflectance is therefore different than the simple surface loss of chemisorbed oxygen due to vacuum in the two tests above.

The reflectance degradation due to ion pump start-up is negligible for wavelengths shorter than 1.0 μ and increases monotonically to 2.4 μ so it appears to be qualitatively equivalent to U-V induced degradation. The reflectance and resistance decreases due to ion pump start-up recover fully and rapidly if oxygen is readmitted, so the

degradation must be restricted to the particle surfaces. This evidence would indicate that ion bombardment degradation and U-V degradation are similar in nature with the former of a smaller magnitude. For example, for a sintered sample after 100 sun-hr at 10 suns intensity, the U-V degradation is 0.3 to 0.4 at 2.0 μ as compared to 0.05 to 0.10 due to ion bombardment. Therefore it would appear at first that ion pump start-up should not seriously affect the interpretation of U-V degradation which clearly dominates except with regard to initial U-V damage kinetics which may be influenced by a surface memory of the earlier ion bombardment.

However, there is evidence that indicates the nature of the ion bombardment degradation may be quite different from U-V degradation. It was shown in Figs. 19 and 20 that a sintered sample irradiated at 10 suns intensity exhibited a gradual 0.15 decrease in reflectance at 2.0 μ over a period of 50 to 100 hr when the sample had experienced no pre-irradiation ion bombardment. In contrast a sample exposed to ion bombardment and then irradiated at 10 suns intensity exhibited a rapid 0.2 decrease in reflectance at 2.0 μ as will be seen in Sec. 5.5 (Fig. 24). The difference in magnitudes and kinetics of the two damage histories indicates that the ion bombardment may have a substantial effect on the surface states which is not evidenced by the relatively small decrease in reflectance which occurs during the ion bombardment. Further evidence of this is provided by spectral irradiation data. Figure 19 showed that for a sample not bombarded by ions, A-H6 radiation filtered by 3-70, 3-71, and 3-72 Corning filters produced less than 0.03 decrease in reflectance at 2.0 μ in 100 hr. Figure 23 shows degradation of a sintered sample irradiated through a 3-69 Corning filter after ion pump start-up. The I-R degradation is significantly greater in 100 hr at 5 suns even though the irradiation transmitted by the 3-69 filter is less energetic than that passed by the 3-70 to 3-72 filter series.

It must be concluded that the ion bombardment does have a very significant influence on the surface stability of the sintered ZnO. The spectral character of the ion effect is strikingly similar to that produced by photon irradiation, but the ion effect must be greater because of the greater degradation subsequently produced by irradiation for those samples which have been ion bombarded.

44
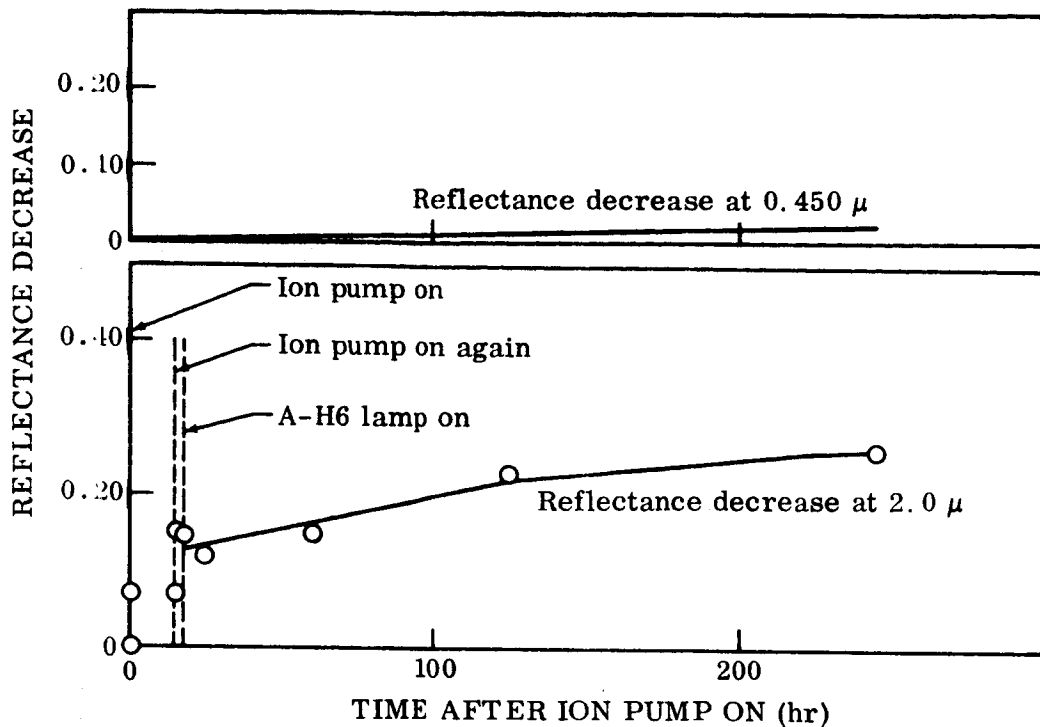
Fig. 23 Decrease in Reflectance of ZnO Due to 3-69 Filtered A-H6 Radiation,
After Treatment by Ion Pump

It is shown in Figs. 24 and 25 that the I-R degradation at 2.0 μ exhibited by S-13 coating is in approximate agreement at several U-V intensities with the sintered pigment which has been ion bombarded prior to U-V irradiation. Both degrade substantially more than the sintered pigment which is not ion bombarded. Hence it would appear that the sintering produces a surface configuration which is markedly more stable than surfaces which result from grinding operations in paint preparation or from heavy ion bombardment during pump-down.

5.5 RADIATION INTENSITY EFFECTS

The effects of intensity are of use for both practical and theoretical purposes. They may be used for evaluating accelerated testing procedures and for determining if the degradation process is a simple one, where one photon produces one hole-electron

LOCKHEED PALO ALTO RESEARCH LABORATORY
L O C K H E E D   M I S S I L E S   &   S P A C E   C O M P A N Y
A   G R O U P   D I V I S I O N   O F   L O C K H E E D   A I R C R A F T   C O R P O R A T I O N

pair, and no interactions are involved. However, the measurement of intensity effects is not the trivial matter it would at first appear to be. It was stated in Sec. 5.4 that there is an effect of the ion pump start-up on the I-R reflectance of sintered samples. The reflectance decreases very rapidly, then increases again slowly with time after the ion pump has started. The increase in reflectance is typically half the damage in the time span of a single day. This raises problems in relation to comparing the kinetics and even the final values of damage due to subsequent irradiation by UV.

First, there is some evidence that the reflectance will decrease more rapidly if the sample being measured has experienced ion bombardment and recovered, than if it either has not experienced ion bombardment, or it has not been allowed to recover before irradiation by UV. All three situations are presented in Fig. 24. The 20-suns intensity test was conducted on a sample that had experienced very little ion bombardment. The 5-suns test sample was heavily bombarded, then irradiated with UV before it had a chance to recover. Finally, the sample irradiated at 1-sun intensity was
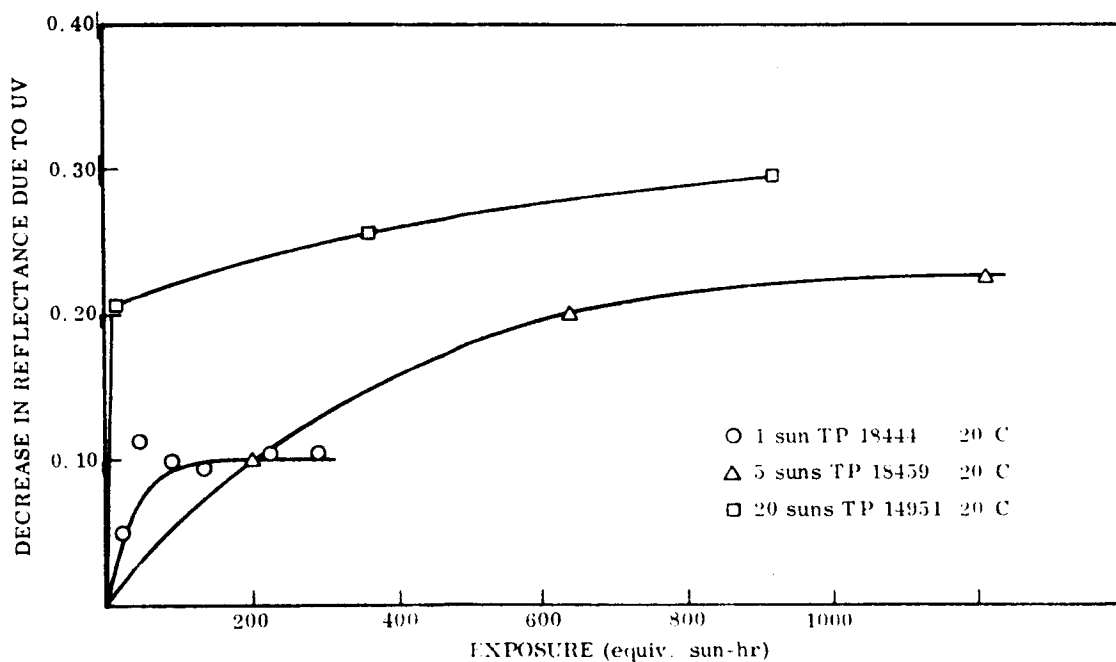

Fig. 24 Decrease in Reflectance at 2.0 μ as a Function of Exposure at 1, 5, and 20 suns Intensity

46

heavily bombarded, then allowed to recover overnight before ignition of the U-V source. The early kinetics of the three curves show no trend with intensity, so it is apparent that the difference in kinetics must be due to the differences in ion bombardment histories.

Second, it is not obvious what zero value of U-V damage should be used in plotting kinetic data. In Fig. 24, it was taken as the value of reflectance measured immediately before U-V irradiation is initiated. This choice, however, may not be the best, as the data for 1-sun intensity will attest. The starting value of reflectance in this test is about 0.05 above the minimum reflectance achieved during pump down. Total damage to the sample at this wavelength (2 μ) was 0.10. These facts may account for the rapid rise in degradation in this sample.

Finally, it is difficult to compare the total extent of damage due to U-V irradiation between samples that have experienced different amounts of ion bombardment. For instance, the 5-suns data in Fig. 24 have a zero point of 0.15 damage, while the zero of damage for the sample exposed at 20 suns is zero. If this is added to the degradation values in the figure, the 5-suns intensity test sample damaged quite significantly more than the 20-suns test sample. This result would be at odds with the trend established between the 1- and 20-sun tests.

Thus, it is clear that attempts to discover the effects of photon flux in this manner may be misleading. Therefore, the effects of intensity on S-13 are included here to represent the effects of the variation of this parameter. It has already been tentatively established that there is little or no effect of the pump on the paint, and that the paint is representative of the pigment (Ref. 15).

The kinetic data for S-13 coating exposed at 1-, 10-, and 20-suns intensity are displayed in Fig. 25. The visible degradation shows little effect of photon flux and depends primarily on the total irradiation. The IR by contrast, shows the same trend as was evidenced by the pigment, i.e., the 1-sun intensity sample damages less than samples damaged at higher intensities. Furthermore, the rate of damage at the higher intensities is greater, even on an equivalent-sun-hour basis.

47
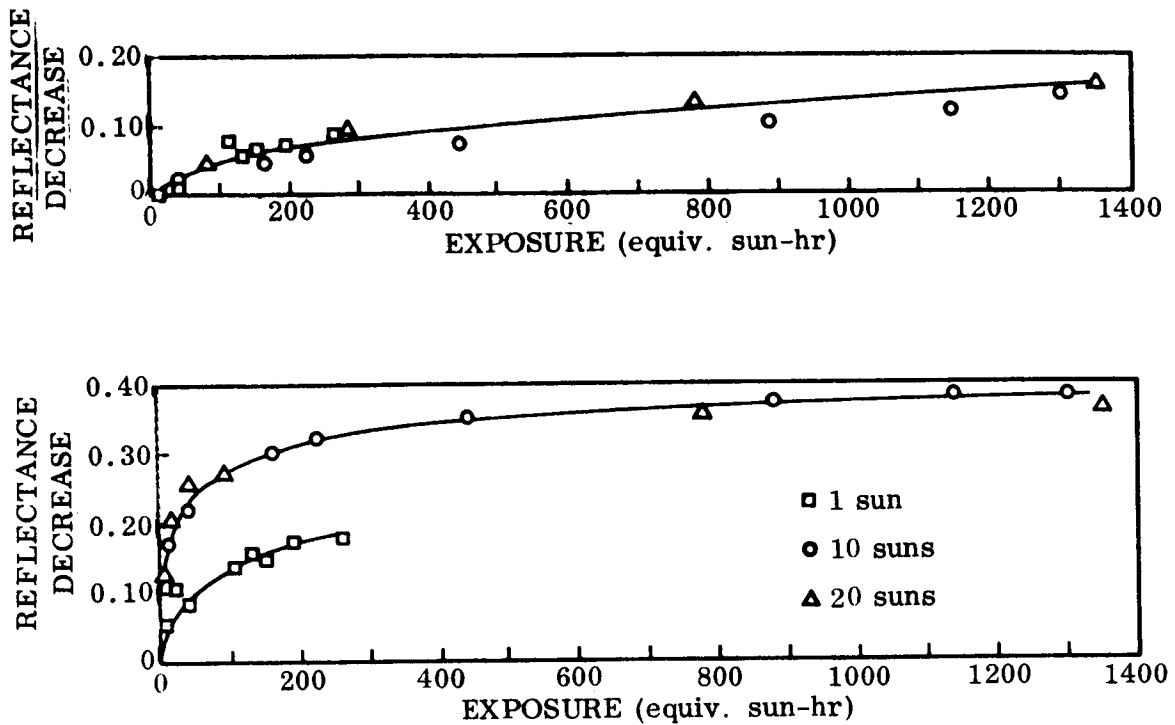
Fig. 25 Change in Reflectance of S-13 at 2.0 and 0.45 μ Versus Exposure, at 1, 10, and 20 Suns Intensity

The results of the intensity variation will not be utilized in the discussion of the model. The model is not at a degree of sophistication yet that data of this sort may be predicted by it.

5.6 U-V DEGRADATION OF SINGLE CRYSTAL

Figure 26 is a transmission spectrum of a single crystal of ZnO which was subjected to U-V radiation at various intensities (3 to 20 suns) for a total of 2900 equiv. sun-hr. The test was performed in a vacuum of 10^{-7} Torr, at room temperature. Absolutely no change in transmission was observed with either before-and-after measurements with the Cary Model 14, or in situ in the bidirectional reflectance apparatus.

A second test has been conducted on a ZnO single crystal — the same crystal, this time at an elevated temperature (200°C). This is a temperature that produces large

48
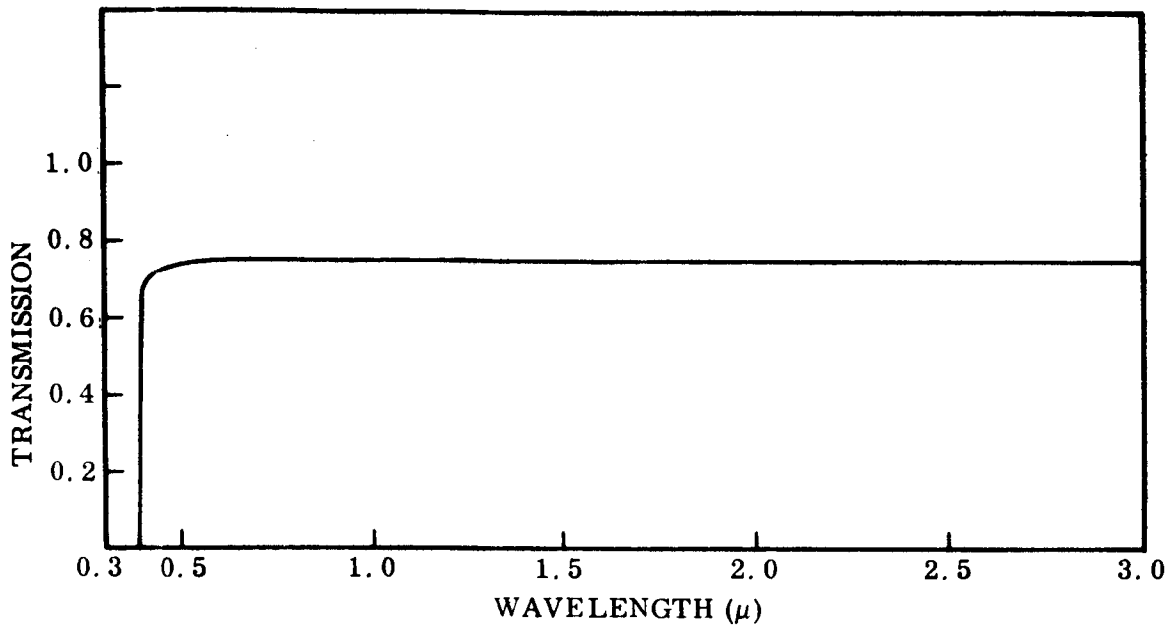
Fig. 26 Transmission of ZnO Single Crystal Before Irradiation and After
2900 equiv. sun-hr Exposure at 20°C

visible damage in the particulate samples. Figure 27 shows that the elevated tem-
perature produced a small amount of visible damage in the single crystal, but still
no I-R damage.

The surface area of a single crystal that is seen by a transmission measurement is
much smaller than the surface area of a particulate sample seen by a reflection
measurement.

Therefore, the lack of damage in the I-R region with the single crystal supports the
previous hypothesis that the I-R damage is a surface effect.

In the visible region, it may first be noted that the same sort of temperature depend-
ence was observed for the single crystals as was observed for the particulate samples.
To this point the results are fairly unambiguous and easily interpreted. However, it
is not entirely clear why there is no observable visible degradation in a single crystal
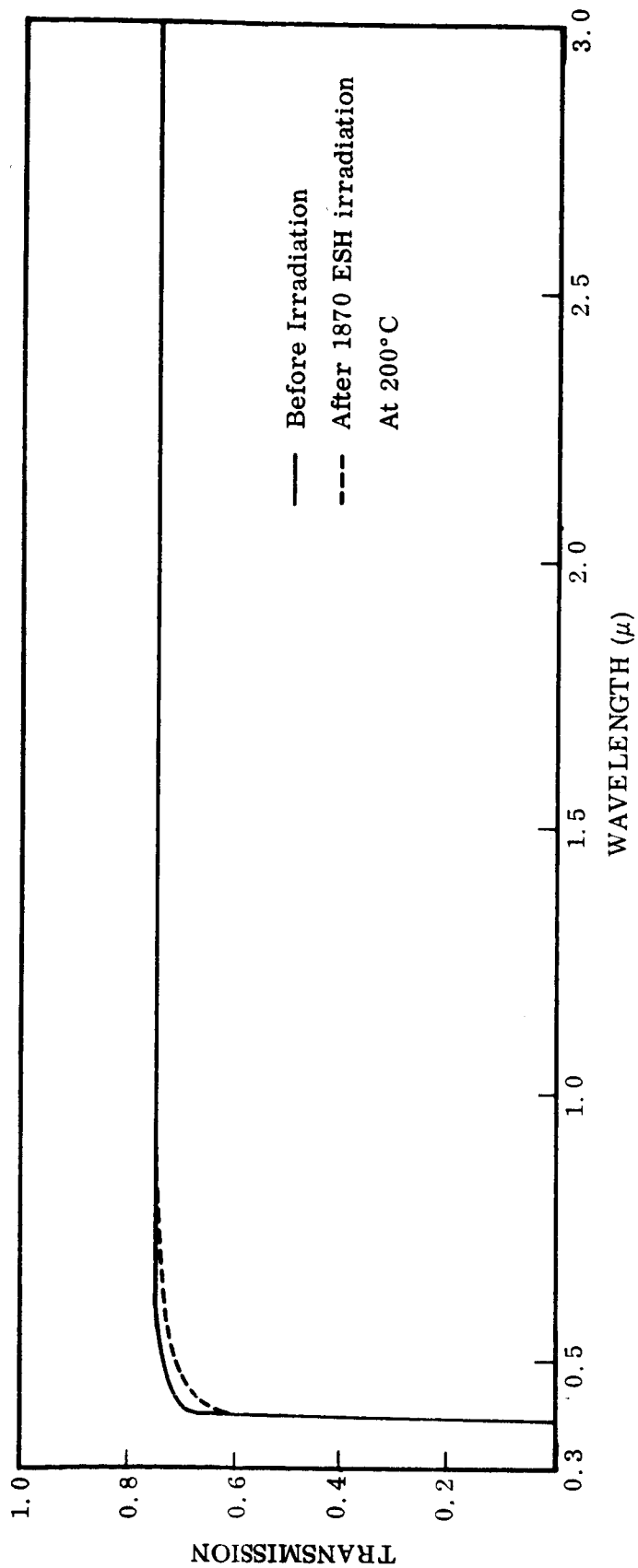
Fig. 27 Transmission of ZnO Single Crystal Before Irradiation and After 1870 equiv. sun-hr Exposure at 200°C

Before Irradiation

After 1870 ESH irradiation At 200°C

WAVELENGTH (μ)

TRANSMISSION

50

at room temperature. At least two explanations are possible, both of which may be correct. It was found in Sec. 5.3 that short wavelength UV ($\lambda < 0.3~\mu$) is required to efficiently produce damage in the visible region of particulate samples. It is known (Ref. 5) that for these short wavelengths the absorption coefficient is so large that no radiation may penetrate further than a fraction of a micron into a crystallite (or crystal) of ZnO. Therefore, we know that in the single crystal the damage is generated near the surface of the crystal.

In the particulate samples, each crystallite is $0.3~\mu$ in diameter. To a first approximation, then, the intensity of a wavefront of short wavelength UV that has entered the crystallite is reduced by a factor of e before it emerges from the other side of the crystallite. Therefore, little short wavelength light will reach the interior of the sample (as distinct from the interior of individual crystallites that compose the sample) by means of transmission through particles; i.e., light will not be transmitted more than a few particle depths into the sample. The reflectance of a highly absorbing crystallite is higher than it would be for a similar crystallite that does not absorb. Nevertheless, it is not expected that short wavelength light will be reflected more than a few particle depths into the particulate sample either.

Thus, it is believed that the visible damage is generated near the surface of both the single crystal and particulate samples. Why, then, is there no damage to the single crystal in the visible, but there is damage to the particulate sample? One possible explanation arises when the above considerations are made somewhat more quantitative. First, it may be observed that typical damage to the visible on a particulate sample is a 5 to 10% decrease in reflectance. Second, the depth of generation of damage in the single crystal may be assumed to be on the order of $0.5~\mu$. Third, the depth of generation of damage in the particulate samples may be $2~\mu$. Thus the (penetrating) light at $0.45~\mu$, which may be taken as a representative wavelength for this region of damage, may have to traverse five or more times the depth of damage in the particulate samples as in the single crystal. Since

$$I = I_o \exp{(-\alpha x)}$$

51

where

I = intensity of transmitted light

I_o = intensity of light that has just entered a particle

α = absorption constant (may be a function of x)

x = depth

The absorbed energy ΔI may be 10^2 times as large for the particulate as for the single crystal sample. This gives a decrease in transmission in the single crystal of $\sim 0.1\%$ — an undetectable change.

This simple theory may not be sufficient. Two assumptions have been made that may not be valid. The samage to the visible region is not, at present, sufficiently well understood to determine whether the assumptions are valid. First, it was assumed that absorption is proportional to the depth to which defects are found. This presupposes the same profile of defect concentration exists in the single crystal or as in the particulate sample, which may not be true. Second, it was assumed that damage is homogeneous at a given depth; i.e., that the damage centers have no tendency to agglomerate. It will be proposed in our model that the damage centers do indeed agglomerate. The energy of the system may be minimized when the damage centers are located in the strain field of a dislocation.

The increase of damage with increasing temperature must be due to an increase in matter transport, from diffusion. However, as before, the details of where the mass is going and why are not clear. It may be diffusion of the centers to a greater depth, or, if the dislocation model is correct, it may be due to transport of the centers to dislocations.

There is a second possible explanation for the difference between the visible damage observed in the crystallites and the single crystal. The dislocation density in the crystallites is likely to be higher than in the single crystal, due to the difference in

52

preparation processes. Thus the difference in damage may be due to a difference in the number of dislocations that are present for the damage centers to migrate to and subsequently produce visible degradation. The temperature effect could then be due to the increased mobility at higher temperature which allows more centers to assume a lower energy position at the dislocations, producing visible damage. It is quite likely that both explanations are valid.

5.7 I-R SPECTRA OF SINTERED SAMPLES

Figures 28 and 29 show the reflectance spectra in the IR for an undamaged sample and a U-V damaged sample. The U-V damaged sample was exposed at about 250°C about 2 yr before its I-R spectrum was measured. The spectrum was measured at ambient conditions, so any changes in reflectance are residual − damage that did not recover upon admission of air to the chamber.
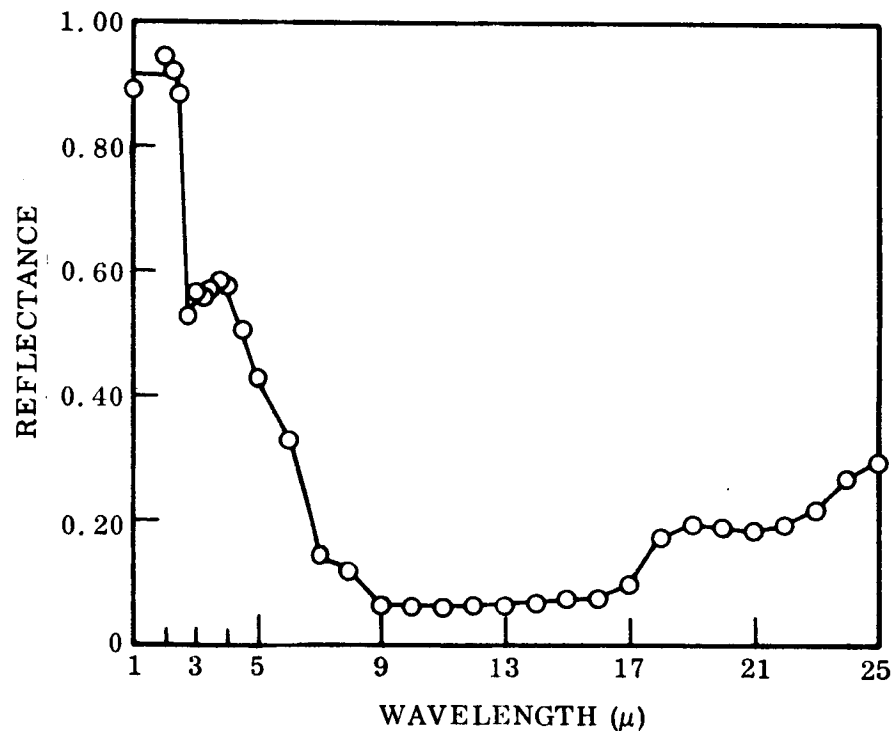
Fig. 28   Reflectance of Sintered ZnO Unirradiated and Pressed at 600 psi

53
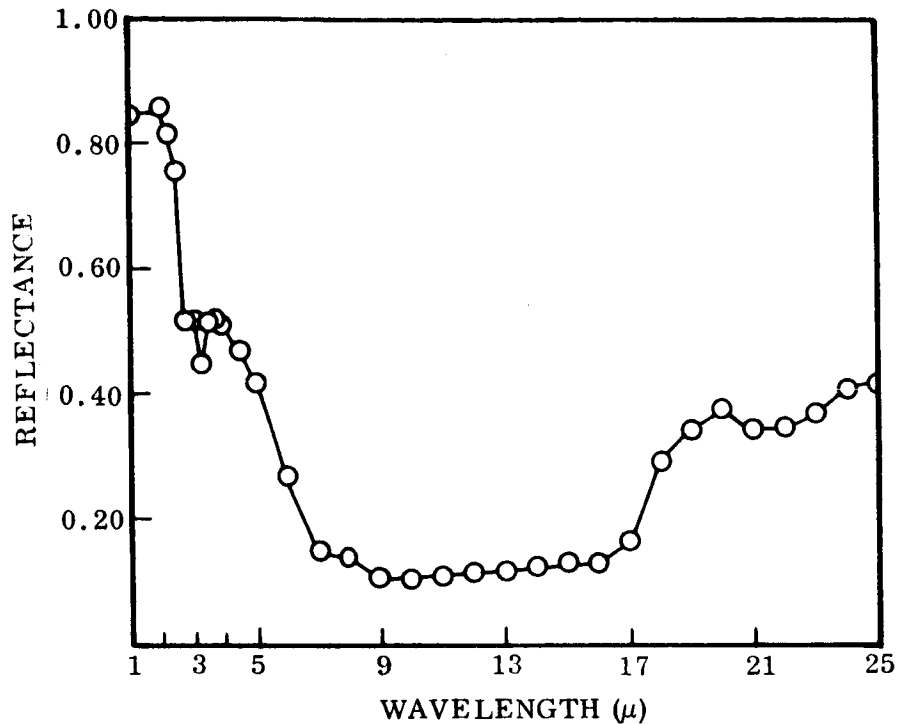
Fig. 29   Reflectance of Sintered ZnO U-V Damaged at
230°C and Pressed at 600 psi

There are five distinguishable spectral areas of absorption in these figures, one near
each of the following wavelengths: 3, 5, 8, 9 – 17, and 21 μ. The region between 9
and 17 μ contains absorptions so strong that no structure can be distinguished. The
absorption at 8 μ is identical in both samples. The absorption at 5 μ is distinguishable
for the undamaged sample, but is not present in the U-V damaged sample. The reason
for this is not obvious. The absorption at 21 μ (0.06 eV) is present in both samples.
The background reflectance around the absorption is different for the two spectra and
thus it is difficult to state unequivocally which sample displays the largest peak. It
would appear that the most reasonable basis for comparison is on a differential basis;
i.e., by subtracting out the background reflectance. On this basis the peak is greater
for the U-V damaged sample than for the undamaged sample. Finally we consider the
absorption near 3 μ. The peaks here do not have the same shape, and do not occur at
the same wavelength. In the undamaged sample the peak appears at 2.7 μ (0.45 eV),

54

which is the location of the water fundamental absorption. The U-V damaged sample
has a broad peak with a sharp peak superimposed at the energy 0.38 eV.

There are really six absorption peaks in the spectrum of the U-V damaged sample,
but the sixth is not easily distinguished. Figure 30 is a plot of the difference between
the reflectance of the U-V damaged sample and the undamaged sample. The
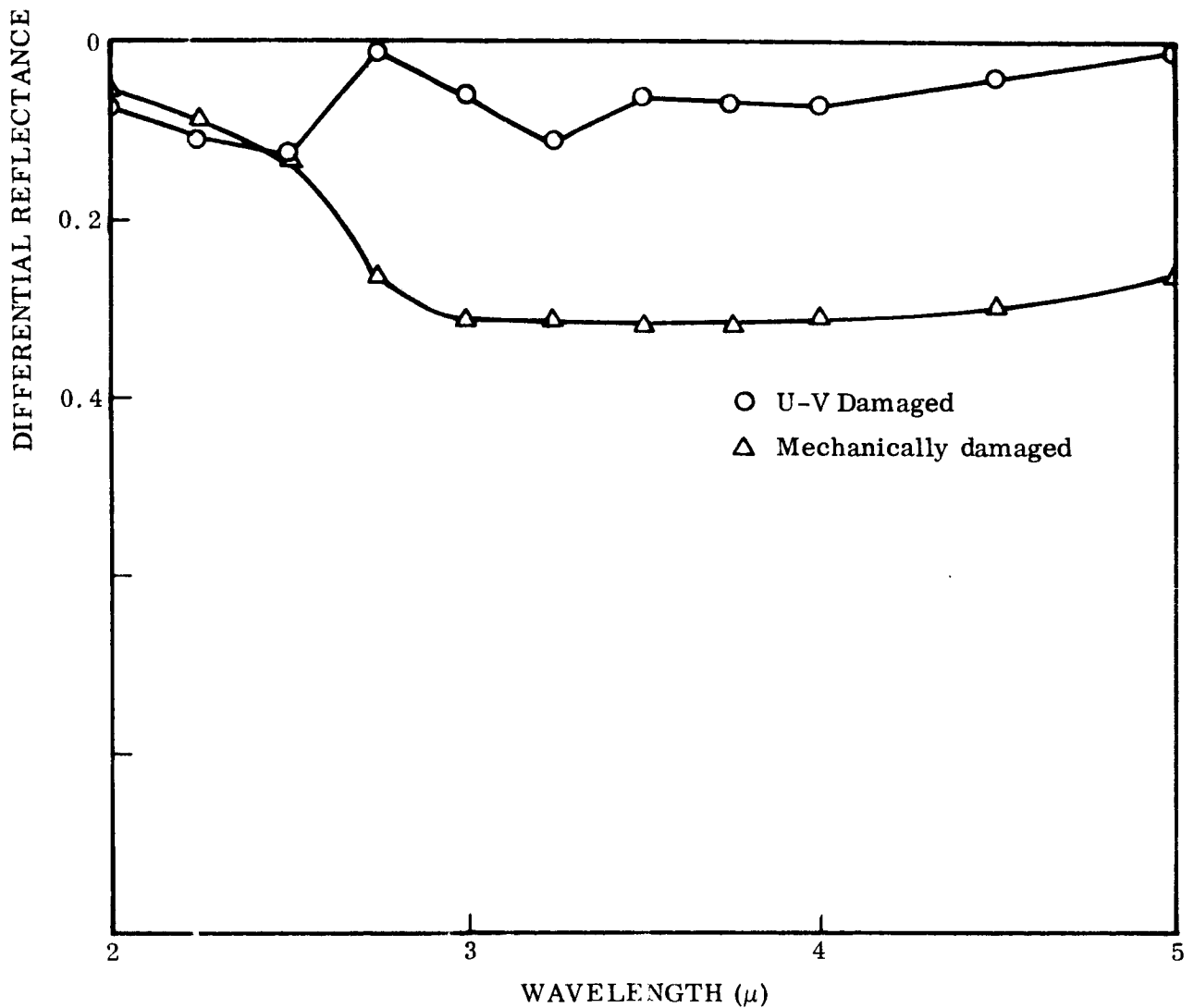
Fig. 30 Difference in I-R Reflectance Between Damaged and Undamaged Samples

mechanically damaged sample will be discussed in the next section. It is seen that there is an absorption produced by the radiation near 2.5 μ. This may also be seen in Fig. 31, which is a representation of spectra taken on a Beckman dual beam spectrometer. The reference that was used was an undamaged ZnO sample.
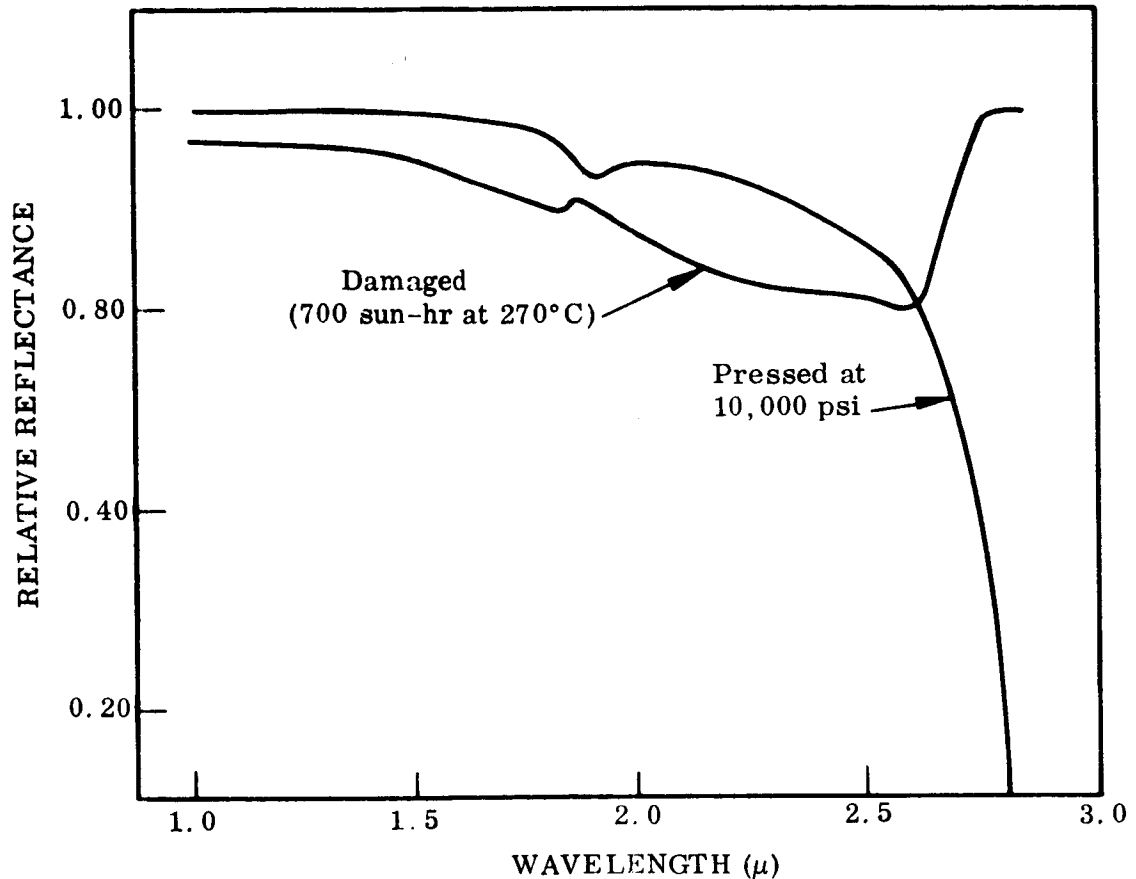
Fig. 31 Relative I-R Reflectance of Sintered ZnO, U-V Damaged and Mechanically Damaged

Both figures show that there is a peak in absorption at about 2.6 μ (0.47 eV). Figure 31 shows that the apparently monotonic decrease in reflectance with wavelength that is typically seen <u>in situ</u> in the IR, and at atmospheric condition for the high-temperature samples, is an absorption peak. The fact that this does not continue to

decrease with wavelength indicates that the degradation is due to a discrete energy level and not to free carrier absorption.

The conclusions reached in this section are as follows:

- There is an absorption at 0.06 eV that increases with U-V irradiation.
- There is an absorption at 0.38 eV that occurs due to U-V irradiation.
- There is an absorption at 0.47 eV that occurs due to U-V damage.

5.8 MECHANICAL DEGRADATION OF ZnO REFLECTANCE

Earlier work (Ref. 15) was done which indicated that the reflectance degradation due to high forming pressures and to U-V irradiation were qualitatively the same in both visible and I-R regions. Furthermore, prior mechanical degradation appeared to result in increased U-V damage. The temptation to associate the damage mechanisms was natural. The effects of high-pressure forming were re-examined following the detection of the absorption peak at 2.65 μ due to U-V irradiation. Samples were pressed at 0, 600, and 20,000 psi, and then sintered at 600°C for 30 min. Reflectance was measured before and after sintering. The I-R reflectance decreased with increasing pressure as shown in Fig. 32, but was unaffected by sintering. Another sample pressed at 20,000 psi was remilled lightly and pressed at 100 psi before sintering. This sample evidenced recovery of I-R reflectance from 0.82 after pressing at 20,000 psi to 0.90 after milling and pressing at 100 psi. These data confirm the observations of Schatz (Ref. 25) on a number of compacted metal oxide powders and his explanation that the reflectance decrease is due to "frustrated total reflectance" resulting from increased compacting and less efficient scattering. He confirms this by also measuring normal transmission of the powders which increased sufficiently to account for the reflectance decrease.

The evidence on visible absorption is more complex. Visible reflectance adjacent to the band edge decreases due to U-V irradiation and slowly but not completely recovers in oxygen. At high forming pressures, stronger absorption occurs at the

57
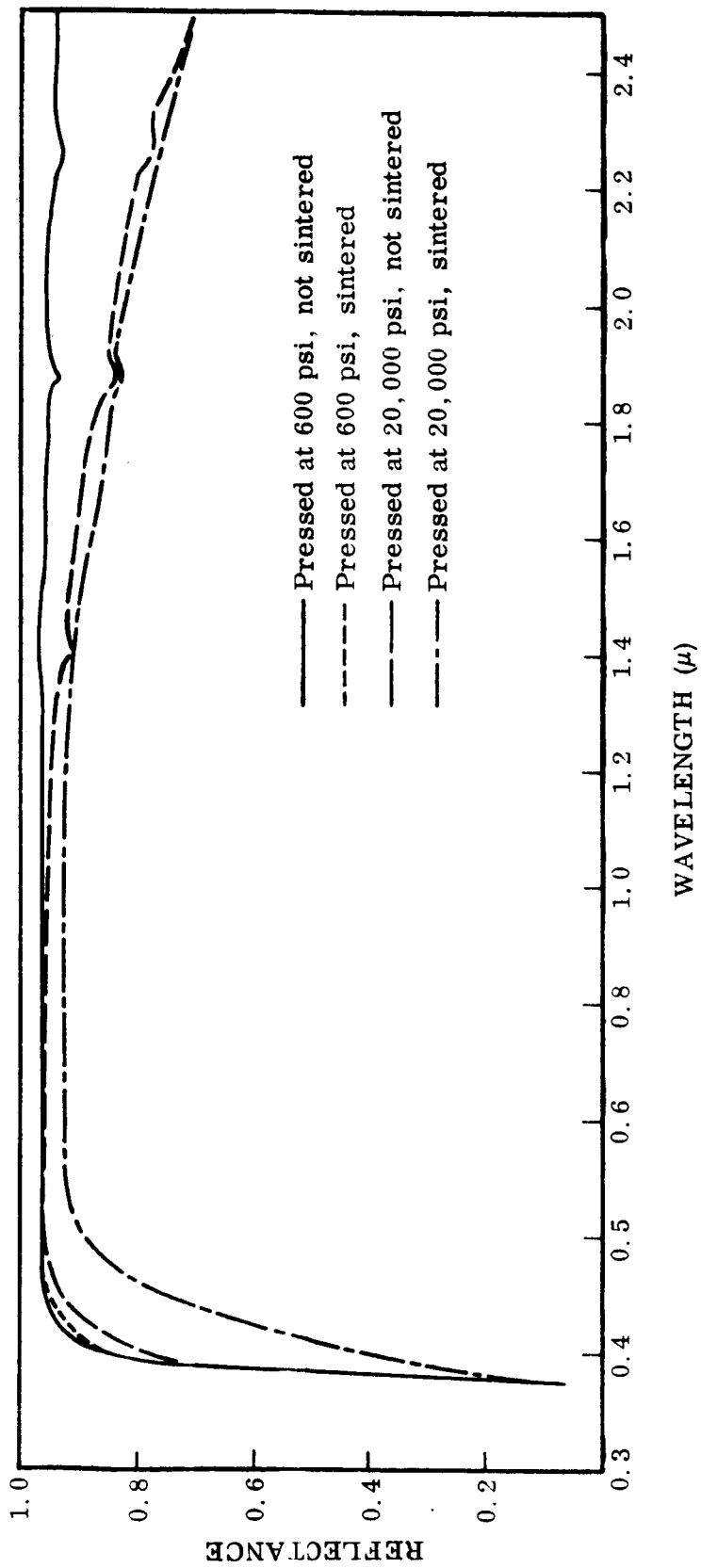
Fig. 32 Effect of Forming Pressure and Sintering on Normal Reflectance

The legend within the figure reads:

— Pressed at 600 psi, not sintered
--- Pressed at 600 psi, sintered
— Pressed at 20,000 psi, not sintered
-·- Pressed at 20,000 psi, sintered

WAVELENGTH (μ)

REFLECTANCE

58

same wavelengths and does not recover. The majority of this absorption occurs during sintering after high pressure forming and is not observed following pressing but prior to sintering. This absorption is strikingly similar to that observed in single crystals heated in zinc vapor (Ref. 26). The solubility of zinc in ZnO is very low [$\sim 10^{12}$ cm^{-3} extrapolated from measurements by Thomas (Ref. 27)] at 100°C and cannot account for the observed absorption. However, it is possible that significantly greater concentrations of zinc atoms or ions may precipitate at defects such as dislocations in the particles, which are probably highly defective particularly after high-pressure forming.

Further evidence that the I-R degradation due to mechanical damage is not the same as that observed for U-V radiation may be derived from Figs. 30 and 31. It is seen that they are quite similar in shape out to 2.5 μ (the long wavelength limit of the Cary reflectance attachment), but that they are markedly different for longer wavelengths.

Figure 33 depicts the spectrum for the far IR for the mechanically damaged sample. There is an increase in the absorption at 0.06 eV, as there was for the U-V damaged sample. The absorption at 8 μ (0.16 eV) is increased over both the undamaged and U-V damaged samples.

The conclusions that have been reached in this section, that are relevant to U-V damage are as follows:

- Infrared damage in the U-V damaged samples is not the same as I-R damage in mechanically damaged samples.
- Visible degradation due to mechanical damage may be the same as U-V induced visible degradation.
- Visible degradation evidently involves diffusion, probably of interstitial zinc to dislocations.
- Absorption at 0.06 eV may be produced by either mechanical or U-V damage.

59
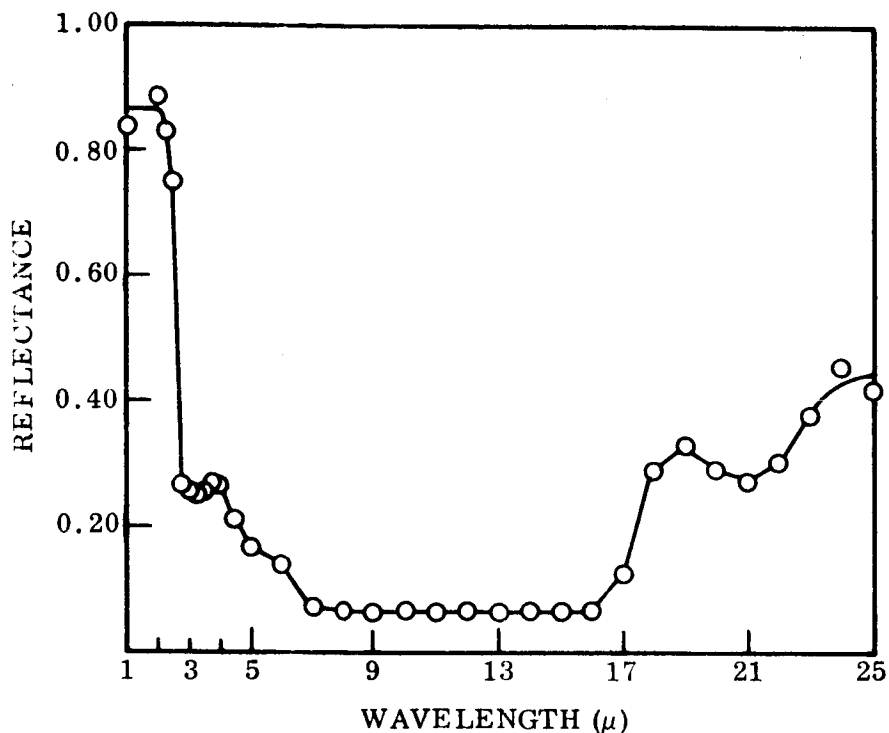
Fig. 33   Reflectance of Sintered ZnO Mechanically Damaged
by Pressing at 20,000 psi

5.9   ESR IN SINTERED ZnO

One effect of U-V irradiation on ZnO is to create paramagnetic centers, both in the
bulk and on the surface.   Electron spin resonance provides a sensitive tool for study-
ing these centers, and hence can be used to gain added understanding of the damage
mechanism.   The intensity of the spin resonance signal is proportional to the number
of paramagnetic centers.   The structure of the line and its g-value give information
on the nature of the center, and a study of the kinetics of formation and decay is
useful in determining the extent to which diffusion and recombination enter the process.
The work discussed here was carried out at liquid nitrogen temperature using powdered
ZnO samples.

60

Figure 34 represents the electron spin resonance signal of ZnO at g = 1.957 (79°K).
Figure 35 is the ESR signal of ZnO at g = 2.001 (77°K). In both figures the first
derivative of the absorption curve is plotted on the ordinate and magnetic field
strength is plotted on the abscissa. The specified magnetic field values were the
points actually measured.

Figure 36 shows the behavior of the spin concentration of ZnO as a function of time
for various treatments. During the first 30 min the sample was pumped down to
10^{-5} Torr. Then it was irradiated intermittently for a period of 70 min. The addi-
tion of air in the absence of radiation produced the tail on the curve. Those data
were taken for the g = 1.957 resonance line.

Fig. 34 Electron Spin Resonance Signal of ZnO
g 1.957 Region at 77°K

61
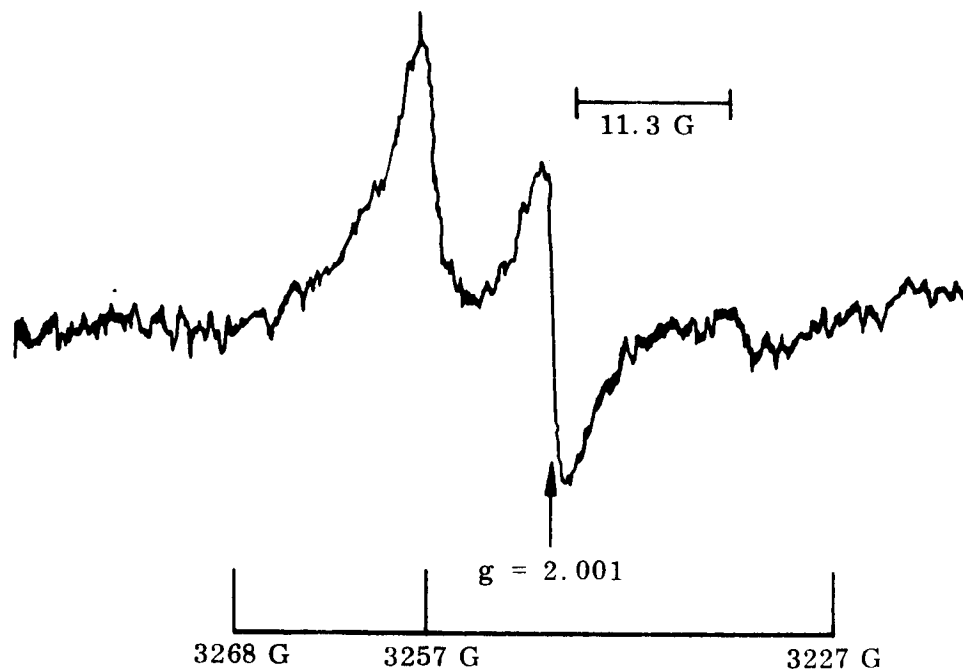
Fig. 35 Electron Spin Resonance Signal of ZnO g $\approx$ 2.001 Region at 77°K
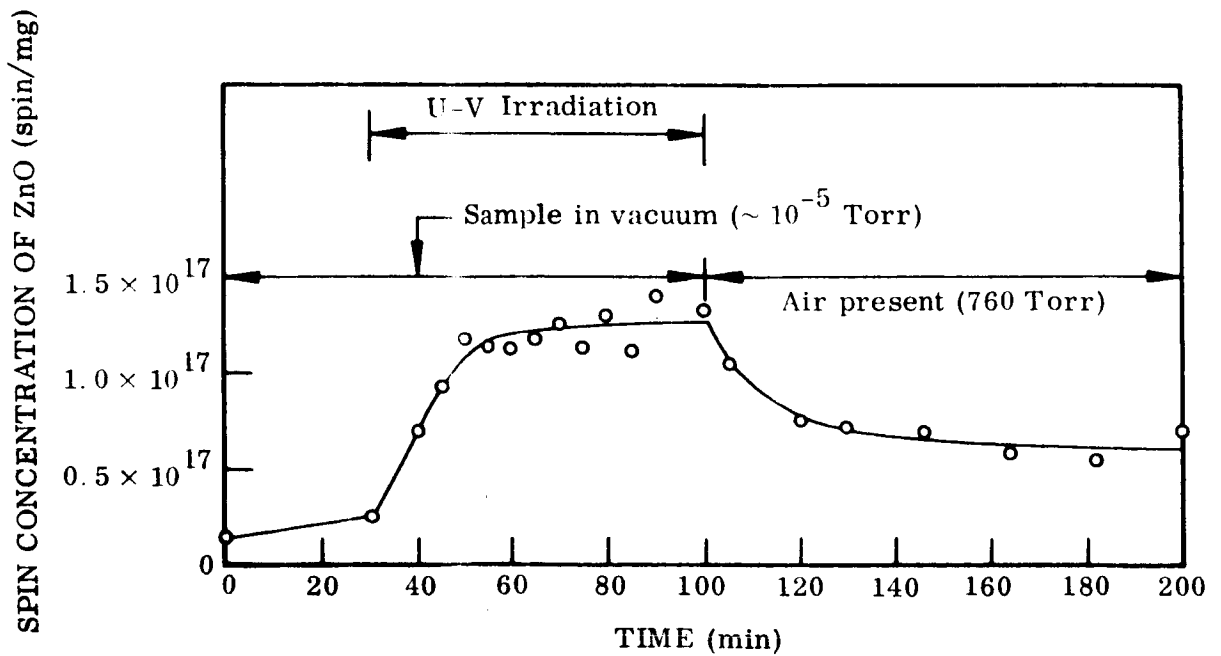
Fig. 36 Kinetics of g $\approx$ 1.957 ESR Line of ZnO at 77°K

62

Section 6

DISCUSSION

In the early work (Ref. 15) on U-V degradation of ZnO pigment it was concluded that optical degradation occurred predominately in two principal spectral regions. The first was in the near IR beginning at $0.8~\mu$ with increasing reflectance degradation at longer wavelengths at least to $2.5~\mu$. The second region was in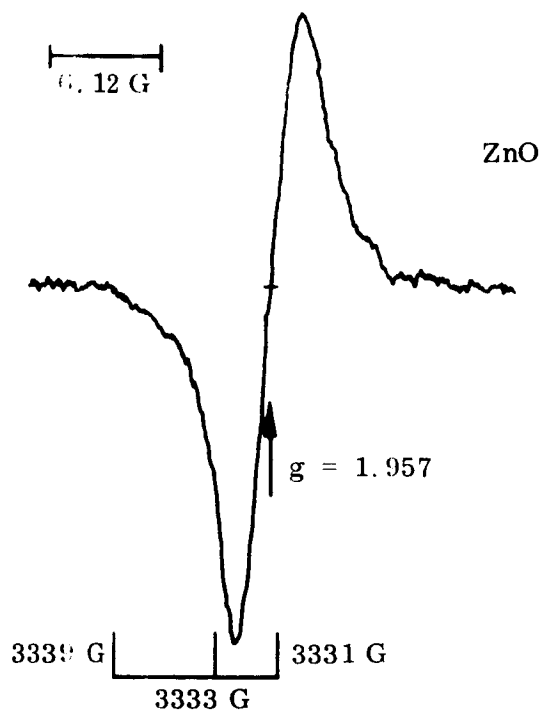 the visible adjacent to the band edge. An example of this degradation is given in Fig. 11. It was observed that the I-R degradation occurred rapidly under irradiation in vacuum and recovered rapidly upon the introduction of air to the chamber. The visible degradation occurred more slowly under irradiation and recovered only slightly in the presence of air. The kinetics of degradation and recovery demonstrates that the two regions of degradation are not directly associated with the same UV-induced defects even though there may be significant relationships between those defects. Consequently this study has quite naturally been divided into separate investigations of the two spectral regions of reflectance degradation.

On the basis of evidence to be discussed, it was decided to concentrate on the identification of details of the I-R degradation during the period covered by this report. This effort has been moderately successful. But as a consequence of this concentration, very little has been learned about specific details of the visible degradation.

An early U-V degradation test on sintered ZnO (Ref. 15) with filtered damaging irradiation established some important tentative results — tentative because the test was conducted without in situ reflectance measurements, and therefore recovery effects could not be accounted for. A sample irradiated with only wavelengths less energetic than band-gap exhibited substantial I R degradation, but no visible degradation. To confirm this result, filtered irradiation tests were conducted with in situ measurements on S-13 coating at the beginning of this contract period (Fig. 21). The two tests gave substantiating results which were as follows: (1) I-R degradation is produced most

63

effectively by wavelengths less energetic than, but near the ZnO band edge and (2) visible degradation requires irradiation by wavelengths shorter than 3000 Å for effective production. Therefore, it is apparent that occurrence of I-R degradation does not necessarily lead to visible degradation unless energetic U-V photons are available, but it is likely that the occurrence of I-R degradation is a necessary pre-condition for the production of visible degradation. These conclusions suggest that the key to understanding the entire U-V degradation process rests on an adequate diagnosis of the I-R degradation. Furthermore, if steps could then be taken to inhibit I-R degradation, visible degradation would necessarily be reduced or eliminated in particulate ZnO.

Based on the foregoing discussion, considerable emphasis was placed on investigating the I-R degradation. These results will be discussed first, and then the few data related to visible degradation.

In the early work (Ref. 15), abundant evidence was collected which related the I-R degradation with loss of oxygen from the ZnO. For example, I-R degradation was easily induced by radiation in vacuum but not in air; the induced degradation recovered rapidly upon readmission of air to the sample chamber. The data did not provide sufficient information to decide if the degradation was due to loss of chemisorbed oxygen or to lattice photolysis and if the absorption was by free carriers liberated by photodesorption of oxygen or by bound electrons at oxygen-related donor states. To acquire additional information, (1) electrical conductivity and spectral reflectance were measured during U-V irradiation, (2) optical measurements were made in a wavelength region not thoroughly covered in the early work, and (3) in separate tests, electron paramagnetic resonance studies were made on sintered ZnO during irradiation and recovery. Important evidence provided by each will be discussed as appropriate.

The role of photodesorption of oxygen in the slow photoconductivity of single ZnO crystals has received considerable attention (Refs. 19--22). To complete the link the

64

spectral photoconductivity of sintered ZnO was measured (Fig. 17). It was then found that I-R degradation was produced by irradiation of the same wavelengths which caused photoconduction. The same minimum photon energy ($\sim$ 2 eV) was required to produce both photoconduction and I-R degradation, and the maximum response of photoconductivity and I-R degradation occurred for approximately the same wavelength ($\sim$ 3800 Å). Two observations may be made about these phenomena. First, it is apparent that both depend on surface processes because of the sensitivity to the oxygen pressure. Second, the maximum interaction of radiation and particles occurs for wavelengths near the band-edge for which the absorption coefficient is small enough ($\sim$ 10 cm^{-1}) to allow penetration deep beneath the sample surface, so that deeply situated particles are irradiated. It is not clear on the basis of existing evidence whether the near band-gap photon must be absorbed near a particle surface to produce a photoconductive or optical change. It is known from data on single crystals that the most effective photons for producing surface photoconductivity are those absorbed near the surface. For the particles the analysis is more complex because the total surface area affected changes with wavelength due to changing absorption coefficient.

Collins and Thomas (Ref. 21) in a study of photoconductivity in ZnO single crystals found that lattice photolysis of oxygen must occur to account for the large observed response. In the work reported here there is considerable evidence to support the contention that a similar lattice photolysis process must be occurring in the particulate ZnO.

Simultaneous measurement of electrical conductivity and spectral reflectance during irradiation of sintered ZnO established that conductivity and I-R degradation were related. The relationship is not simple because (1) conductivity of sintered powders is dependent on particle-to-particle potential barriers due to band-bending at the surfaces as well as the number of free carriers and (2) the reflectance of a scattering matrix cannot be directly related to the fundamental property – absorption. Hence, it is fruitless to attempt a quantitative description of the conductivity-reflectance relationship. Nevertheless the kinetics of conductivity and I-R reflectance changes during irradiation and recovery reveal important evidence. The large increase in dark

conductivity due to evacuation (Fig. 17) is not accompanied by a decrease in I-R reflectance. Upon initiation of U-V irradiation the reflectance does not decrease until the conductivity is near its maximum value (Fig. 12). These data indicate that upon evacuation of the chamber chemisorbed oxygen leaves the surface liberating carriers and reducing the band-bending at the particle surfaces. The time of ~ 1 hr to establish an equilibrium drak conductivity in vacuum indicates that the binding energy for the chemisorbed oxygen is near 0.03 eV. Since increased I-R absorption is not simultaneously observed, the absorption is not related to states associated with chemisorbed oxygen. This has been obtained.

It is not clear on the basis of the simultaneous electrical and reflectance data whether the I-R absorption is due to free carriers liberated by lattice photolysis or to bound states associated with the resultant oxygen vacancies. Even though the conductivity nears a maximum before optical degradation begins, if the conductivity is controlled by particle surface barriers, then there is no way to evaluate the population of free carriers. The indication is that the absorption is associated with bound states which are produced following the liberation of large numbers of carriers which produce no significant I-R absorption, but supplementary information is needed to confirm this hypothesis.

In situ reflectance measurements are limited to wavelengths shorter than 2.5 μ. Ultraviolet induced absorption increases up to 2.5 μ, and it cannot be definitely determined if the increasing absorption is characteristic of free carrier or bound state absorption. To resolve this, reflectance measurements were extended to longer wavelengths with other spectrophotometers. This required using a sample damaged at high temperature, which exhibited residual I-R degradation after a long period under ambient conditions. The reflectance of this sample relative to undamaged ZnO exhibits one or more minima in the vicinity of 2.8 to 3.2 μ (Figs. 30 and 31). These minima are indicative of bound-state, not free carrier, absorptions. It should be noted that the sample for which these spectra were measured was irradiated at high temperature and thus oxygen vacancies could diffuse away from the particle surface during irradiation, and not be refilled during recovery. Even though the residual damage is characterized by bound-states, that does not rule out the possibility that

66

during irradiation the I-R absorption is partially due to free-electrons and partially to bound states associated with oxygen vacancies. However, due to the general shape of the I-R absorption which closely resembles that in Fig. 12 for all damage spectra it is evident that the major portion of the I-R absorption is attributable to bound states.

Additional evidence pertinent to identification of the I-R absorption was obtained through electron spin resonance studies.

The electron spin resonance spectra observed in samples of ZnO sintered particles, as shown in Figs. 34 and 35 are in general agreement with the results reported by other workers (Refs. 28−34). The resonances observed in the vicinity of g ≃ 2.06 typically showed an symmetric line shape and some structure, indicating the presence of more than one unresolved resonance. These lines were very sensitive to the presence of oxygen and the previous treatment given the sample. Their behavior was not completely reproducible from sample to sample. A partial explanation of this was the inadvertent variation in previous treatment given the sample. These resonances with g > 2.00 are generally attributed to various species of adsorbed oxygen (Ref. 34). The U-V sensitivity of these centers can vary greatly and also depends on the heat treatment given the sample.

In this work we focused our attention on the line at g = 1.96, shown in Fig. 34. There exist in the literature conflicting interpretations regarding the origin of this resonance. It has been suggested that the line observed is due to bound electrons at a donor (Scheider and Raüber, Ref. 28; Baranov, Kholmogorov, and Terenin, Ref. 32; Kasai, Ref. 29) or mobile electrons, either in the conduction band or in a shallow donor band (Müller and Schneider, Ref. 30; Kokes, Ref. 31). In most cases this resonance has been found to be sensitive to U-V irradiation. However, in the samples studied by Kasai U-V irradiation caused a slight decrease in intensity. Geisler and Simmons (Ref. 6) have suggested that more than one kind of paramagnetic center, with a resonance at g ≅ 1.96, can exist in ZnO. One of these, that studied by Kasai, is present in samples which have been heat-treated at high temperatures (ca. 975°C). This resonance is relatively insensitive to UV. The resonance which we studied also occurs

67

at g = 1.96 and is sensitive to U-V irradiation, as indicated by the plot of increasing intensity with time of irradiation (Fig. 36). We believe that this resonance is due to mobile electrons in the crystal. The fact that the g-value is less than the free electron g-value indicates that holes are not responsible for the resonance. It is not possible to ascertain without further information whether the electrons are in a donor band or in the conduction band. It is very possible that electrons in both bands are contributing. The fact that no observers have ever detected a hyperfine splitting due to Zn^{67} (I = 5/2), either in powder or single crystals, is evidence that the electrons responsible for the resonance are not localized.

The experimental evidence can tentatively be explained by the following mechanism. The incident U-V and visible radiation causes oxygen to be evolved from the ZnO particles, initially from the surface and then from within the bulk of each particle. The oxygen vacancies created act as donors, and hence the intensity of the resonance increases as more oxygen is released. Existence of the resonance under illumination in air, with an intensity reduced from that obtained in vacuum, represents establishment of a steady state in which oxyten is being both evolved and reabsorbed into the solid. When air is admitted to a sample chamber which has been irradiated in vacuum the intensity of the resonance drops. However, in the absence of further irradiation the signal does not drop back to the vanishingly small value observed in unirradiated samples. We attribute this to the fact that oxygen on the surface first fills oxygen vacancies near the surface, and consequently further diffusion from the surface to vacancies in the bulk is inhibited, resulting in a greater equilibrium number of vacancies.

The resonance at g $\simeq$ 1.96 observed by Kasai may in fact be due to a different paramagnetic center than what we observe, as suggested by Geisler and Simmons. However, a great many apparently contradictory facts remain to be resolved before this problem is understood.

A summary of the experimental evidence related to visible degradation makes it obvious that the visible and I-R degradation are grossly different. First, although the

68

evidence is not conclusive, it appears that I-R damage must occur before visible damage can proceed. Second, the energetic UV ($\lambda < 3000$ Å) is required for significant production of visible degradation. This requirement explains why no visible degradation is caused by ion pump start-up in the dark (Fig. 22). Whereas there are definite correlations between I-R degradation and complementary measurements of electrical conductivity and ESR spin concentrations, no such correlations are established for the visible degradation. This is not surprising because the visible absorption must be due to an acceptor rather than donor state or to a lattice distortion and therefore cannot contribute significantly to conductivity in n-type material. In addition, since the visible absorption is produced by photons which are absorbed completely in the first few particle depths, the number of absorption sites must be very small compared to the number of I-R absorption sites produced at the multitude of particle surfaces irradiated by the weakly absorbed visible photons. The few visible absorption sites required for detection is verified by the single crystal irradiated at high temperature (Fig. 27). With a single surface sufficient defects are produced to observe an absorption shoulder in the visible.

The location and shape of the U-V induced visible absorption are similar to that produced by high pressure forming followed by sintering. Both of these are reminiscent of absorption produced by excess zinc diffused into the lattice (Ref. 26). The fact that sintering at 600°C is required before substantial visible degradation due to pressing occurs indicates that a diffusion process is involved. The solubility of zinc in the lattice is small (Ref. 27) so it may require precipitation of zinc at defects to produce significant absorption. That the visible degradation apparently requires a diffusion process is evidenced by the single crystal irradiation experiments which required high sample temperature to produce measurable absorption. Early work (Ref. 15) on sintered samples shows a very strong effect of temperature on the magnitude of visible degradation. It is possible that the energetic UV is required to ionize zinc atoms so that they can start diffusing from the particle surface into the bulk. However, the lifetimes of the ionized state are so short, that significant diffusion could not occur if maintenance of the ionized state were required thereafter. The very slow and limited recovery of visible absorption sites indicates that they reside in the particle

bulk. Further it is likely that these defects are associated with neutral zinc atoms, because if ionized they would be influenced by Coulombic attraction to the negatively charged surface and would diffuse out. Furthermore, the singly ionized state is a donor state which cannot produce visible absorption and the doubly ionized state has most probably an extremely short lifetime.

If a diffusion process is required for visible absorption to result, the times involved are short. The kinetics of visible degradation (Fig. 25) indicate that degradation starts nearly at the initiation of irradiation or within an hour afterward. If such a short diffusion time is required it is not clear why irradiation in the presence of air (Fig. 13) did not promote the reverse process, visible recovery. The explanation for the irreversibility of visible degradation may relate to the expectation that the sites of the excess zinc in the particle bulk are stable sites at lattice defects.

70

Section 7
WORKING MODEL FOR U-V DEGRADATION

Prior studies of the interaction of electromagnetic radiation with ZnO have emphasized the complexities of the degradation mechanisms. A complete theory has yet to be formulated. However, the goals of this program have been the formulation of a reasonably firm hypothesis for the degradation in optical properties of one spectral region and an attempt to relate previously unrelated experimental results. It is thought that the mechanism for degradation in the I-R spectral region is understood and that some definite statements may be made about the degradation process in the visible spectral region of ZnO pigments.

The process of degradation to the optical properties of ZnO particulate samples may be outlined as follows: damage is initiated by the absorption of a photon by the ZnO crystallite; the absorption process must involve the creation of a hole-electron pair; some portion of the U-V created holes may migrate through the particle.

The surface of each particle has chemisorbed oxygen on it. The oxygen has become chemisorbed by trapping a lattice electron, creating negatively charged surface states. There is a compensating depletion layer inside the semiconductor. This depletion layer may be described by the bending of the bands upward toward the surface.

The radiation-produced holes are attracted to the surface by the potential gradient described by the bent bands. At the surface recombination takes place between the trapped electron on the oxygen and the itinerant hole.

When a hole recombines with a trapped electron on an oxygen state, it neutralizes the oxygen, thus changing it from the chemisorbed state to the physically adsorbed state. Physically adsorbed oxygen is only lightly bound, and may be thermally desorbed.

71

Ultraviolet radiation has, then, caused oxygen to leave the surface. The resultant surface obviously has a higher concentration of zinc than previously. From this point in the development it is necessary to show how this zinc-rich, oxygen-depleted surface may result in decreases in reflectance in the visible and I-R spectral regions.

The absorption in the IR is considered to be caused by states near the conduction band, on the surface of the particles, caused by surface oxygen vacancies. It is proposed that these states absorb I-R photons through the excitation of electrons to the conduction band. The number of these states will increase, as will the population, due to irradiation in vacuum. Admission of oxygen will immediately remove most of the states, and depopulate those that are left through the upward bending of the band.

The absorption in the visible is not as well understood as that in the IR. A model has been proposed that fits all data observed, but there is not enough evidence to present the model with a great degree of confidence.

It is suggested that some of the excess zinc on the surface may diffuse into the bulk of the particle and create high zinc concentrations around dislocations. This increase in concentration would increase the lattice distortion in that region. Regions of distorted lattice will change the band structure locally, reducing the band gap in the case of lattice expansion of ZnO considered here. The result is absorption of less-than-normal-band-gap radiation and a decrease in reflectance in the visible spectral region.

Models have now been suggested for the progression from the absorption of a photon and the creation of a hole-electron pair to the creation of absorption centers that will produce decreases in reflectance in the two characteristic spectral regions. These models must next be examined in the light of the experimental data available.

The strongest absorption of photons occurs for energies greater than the band gap. However there is evidence that photons are also adsorbed for $0.4 < \lambda < 0.6 \mu$ in undamaged particulate samples, as well as U-V damaged samples. The absorption is not detectable by optical measurements before irradiation, but spectral photo-conductivity measurements show that hole electron pairs are, nevertheless, created.

72

There are three possible explanations for an absorption in this region. There may be a continuum of states up to 1 eV below the conduction band, thus creating the observed absorption through excitation from the valence band to these states. There may be a continuum of states up to 1 eV above the valence band, thus creating the observed absorption through excitation from these states to the conduction band. Finally, there may be localized regions where the band gap is not as large as it is in the bulk of the particle.

If excitation is to occur from the valence band to states beneath the conduction band, these latter states must be empty. But it is known that in single crystals of ZnO under ambient conditions that the Fermi level is within a fraction of an electronvolt of the conduction band, and thus these states must be filled. Parenthetically it may be observed that very little visible damage is incurred by single crystals, which would be consistent with the Fermi level location in the bulk if this explanation were valid. In the pigments under consideration, however, essentially the entire particle may be considered to be surface, since they have a 1500 Å radius and the surface may be considered to extend on the order of 1000 Å toward the center of the particle. The bands at the surface are known to bend above the Fermi level, probably on the order of 1 eV. Thus states below the conduction band may be available for excitation of electrons from the valence band in crystallites. Up to this point, the existence of states below the conduction band provides no contradictions. However, if it is now desired to assign the visible damage to them, it is found that a contradiction does arise and they must be eliminated from consideration. Continued irradiation of ZnO particles will cause most of the surface oxygen to leave, and thus the bands to flatten, and possibly even bend down as the surface becomes zinc rich and positive surface states are created. In this case the states beneath the conduction band would no longer be available for excitation from the valence band, and no visible degradation would be observed in situ. Furthermore, the optical properties in this spectral region would be highly sensitive to oxygen pressure. Neither circumstance is observed, and thus this possibility must be eliminated.

The second possibility, that of sites above the valence band, cannot be so summarily dismissed. This mechanism does create the problem that the holes are left on the localized states above the valence band until the hole is excited to the valence band, but it cannot be dismissed on this basis, since thermal excitation of the holes to the valence band is possible. A hole thus localized is not completely free to migrate to the surface, liberate oxygen, and cause the observed changes in properties. If this mechanism were valid, it would be expected that long wavelength radiation simultaneous with less-than-band gap radiation would efficiently produce itinerant holes and thus optical damage. The role of the long wavelength radiation would be to excite the holes from the bound states to the valence band. This experiment has not as yet been performed. The diffusion length for holes has been estimated to be on the order of 4×10^{-5} cm, which is greater than the average diameter of the ZnO particles. Thus there is a substantial probability that photon-induced holes will diffuse to the surface, once they are generated, and are in the valence band.

The argument against the second possibility does not eliminate it in favor of the third possibility, especially since the same arguments, to a considerably lesser degree, may be applied against the third alternative. However, it may be said that the third explanation is preferred on the basis of the above, and because no evidence exists for the presence of states above the valence band, while evidence does exist for lattice distortion. Lattice strain has been observed by x-ray diffraction techniques to exist in highly zinc-doped ZnO. This strain may produce a region of the crystal with a smaller band gap than the rest of the crystal possesses, and thus absorption for longer wavelengths. Zinc oxide at ambient conditions already is near saturation in zinc content. Thus strain due to interstitial segregation may exist prior to irradiation, causing photoconductivity response. The role of the radiation, then, is to increase the concentration, and thus the distortion, so that the absorption becomes strong enough to be detected with optical measurements. The increased concentration at the dislocations would result if the excess zinc at the surface of the particles diffuses into the bulk of the particles, then migrates preferentially to dislocations. The total strain of the lattice is reduced if the concentration of interstitials is higher around dislocations than in otherwise unstrained portions of the lattice. This fits the observation that the

visible degradation involves diffusion. Further, it is possible to devise a mechanism on the basis of this model whereby long wavelength radiation and short wavelength radiation are both needed (simultaneously or the latter subsequent to the former) to produce the visible degradation, while neither will efficiently produce it by itself.

Hole-electron pairs will be created with greatest efficiency by greater-than-band-gap energy photons. However, this process is restricted to the first layer or two of particles by the high absorption coefficient for these photons. For less-than-band-gap radiation transmission and scattering processes will allow for pair generation and subsequent oxygen desorption to occur over a depth of tens or hundreds of particles. Thus it is to be expected that the effective degradation of an entire sample will be most strongly influenced by radiation of slightly less than band gap energy. Even though the quantum yield for pair generation is less than that for band gap energy, the surface area available for damage more than compensates for the reduction in efficiency when viewed in terms of changes in reflectance.

The role of $\lambda < 0.3\,\mu$ radiation may only be guessed at for the present. One possibility is that the high-energy radiation ionizes neutral zinc and allows the atom thus decreased in diameter to diffuse more rapidly. This may be a diffusion within the surface particles, or it may enable the surface zinc to enter the particle.

The far I-R reflectance data show an absorption of 0.05 eV. This energy is characteristic of the first ionization of interstitial zinc. This lends support to at least the existence of the interstitial zinc in significant quantities in ZnO; and the increase in the size of the peak after irradiation supports the theory that interstitial zinc concentration increases due to U-V irradiation. The consequent increase in visible absorption is a possible conclusion following this observation.

The loss of oxygen from the lattice does not proceed at a constant rate. Initially the degradation process as manifested by the liberation of oxygen proceeds rapidly, with holes being accelerated to the negatively charged surface. Eventually the rate decreases and becomes limited by the probability that holes can overcome the retarding

potential created by the surface that has become positively charged due to the excess zinc. The results of Collins and Thomas (Ref. 21) confirm this for single crystals of ZnO. This would indicate that eventually the degradation will saturate as the rate of readsorption of oxygen from the ambient atmosphere becomes equal to the rate of arrival of holes at the surface. This is observed in terms of saturation of the optical degradation.

The I-R spectra also shows two absorptions created as a result of U-V irradiation with energies near 0.4 eV. This is near the energy associated with a doubly ionized oxygen vacancy in the bulk of a ZnO single crystal. It is not unreasonable to suppose that a similar center on the surface of a crystallite give rise to at least one of the observed absorption peaks. Thus it is believed that the I-R absorption observed in situ is a broadening of one or both of the absorptions observed after irradiation, at atmospheric pressure. These absorptions are believed to result from surface states below the conduction band caused by surface oxygen vacancies. Among other things, this hypothesis has the desirable quality that both the presence and occupation of the states are highly sensitive to ambient oxygen pressure. The states may be filled and emptied by the bands bending down and up respectively, and they are created and destroyed by removal and addition of oxygen. Both phenomena agree with the observed pressure dependence.

The I-R absorption has been shown to be directly related to the loss of lattice oxygen from the growth and recovery kinetics of both the reflectance damage and electrical conductivity. There are two explanations for the absorption that have been suggested: free carrier absorption and states beneath the conduction band, herein attributed to oxygen vacancies. It is possible to remove the former from further consideration. The evidence of the absorption spectrum just cited is convincing, but is not conclusive. It is possible that both the discrete levels and the free carrier absorption exist in situ. The argument for this would assume that when oxygen is admitted to the irradiation chamber, the bands bend upward on the ZnO particulate samples as oxygen becomes chemically adsorbed. The oxygen would therefore localize the free carriers that had produced the bulk of the absorption in situ and the measurements made in the far IR

76

would not be able to detect the presence of the carriers. Only the discrete levels below the conduction band would be left at the time of the measurements, which are made at atmospheric pressure.

There are two arguments, however, that exclude the possibility of the I-R absorption observed in situ being free carrier absorption. First, free carrier absorption would manifest itself as an absorption that increases as the third power of the wavelength (Ref. 35). The observed dependence is more nearly proportional to the first power of wavelength. Second, from the electron spin resonance work, it is known that no significant g-value characteristic of free electrons was observed for reasonable intensities, while a strong signal was observed for a bound state created by the UV.

The other explanation, that of oxygen vacancies creating surface states below the conduction band, is quite compatible with all the above experimental data.

It has been shown that the model for degradation of particulate ZnO fits all the observed data that seemed relevant, and that it is self-consistent. The qualitative features of the model for the I-R degradation appear to be reasonably well confirmed, and it would seem, at the present time, to be correct. The degradation in the visible region is not as well understood, and is presently thought to be a more complicated phenomenon. The proposed model fits the observations to date, but the experiments have not been completely definitive. Therefore this portion of the model must be considered to be quite preliminary.

The model proposed here is tentative in the sense that it leaves several questions open for further investigation. It has been designed as a means of coordinating the known properties of ZnO into a coherent and self consistent picture. The complexity of the system precludes the possibility of a definitive model at this time, and no quantitative statements may be made.

77

Section 8
CONCLUSIONS

The following conclusions result from the work discussed in the preceding sections:

- Solar-radiation-induced degradation of particulate ZnO reflectance occurs in two spectral regions – the visible adjacent to the band-edge and the near IR between 0.8 and 2.8 .

- Infrared degradation and photoconductivity are produced most effectively by the same photons, those less energetic than, but near the band-gap of ZnO.

- Visible degradation is most effectively produced by photons of wavelength less than 3000 $\overset{\circ}{A}$. It is not certain, but probable, that the occurrence of I-R degradation is a necessary precondition for production of visible degradation.

- The kinetics of I-R degradation are strongly dependent on the irradiation intensity as well as the total irradiation. The visible degradation is primarily dependent on the total irradiation.

- The glow discharge which accompanies start-up of an electronic vacuum (VacIon) pump may cause significant I-R but no visible degradation of sintered ZnO.

- The I-R degradation is strongly affected by surface preparation of the ZnO particles. Samples sintered, sintered and exposed to VacIon start-up, and milled into a paint, exhibit progressively more total degradation during irradiation.

- Recovery of I-R degradation is very rapid and complete when the irradiated ZnO is introduced to oxygen. The recovery of visible degradation is slow and incomplete.

- Recovery processes are not significantly affected by selective wavelength irradiation of the degraded ZnO during recovery.

78

- Changes in electrical conductivity and ESR spin concentrations are related to the I-R degradation, but not to the visible degradation.

- Irradiation of a single crystal at high temperature caused a decrease in visible transmission, but no effect in the IR. Irradiation at room temperature produced no observable degradation in either region.

- The working model for solar-radiation-induced damage to the optical properties of ZnO has been revised to accommodate the foregoing results.

- The U-V induced I-R absorption is attributed to bound donor states associated with oxygen vacancies which reside at the particle surfaces the preponderance of evidence excludes a significant contribution by free carrier absorption.

- The visible absorption is tentatively attributed to localized changes in bandgap due to lattice strain or to states up to 1 eV due to lattice strain or to the valence band associated with zinc which has diffused into the particle bulk and precipitated at lattice defects.

Section 9

REFERENCES

1. Lockheed Missiles & Space Company, <u>Thermophysics Design Handbook</u>, Report 8-55-63-3, Sunnyvale, Calif., Jul 1963

2. R. E. Gaumer and L. A. McKellar, <u>Thermal Radiative Control Surfaces for Spacecraft</u>, LMSC-704014, Lockheed Missiles & Space Company, Sunnyvale, Calif., Mar 1961

3. R. L. Olson, L. A. McKellar, and J. V. Stewart, "The Effects of Ultraviolet Radiation on Low α_s/ϵ Surfaces," Symposium on Thermal Radiation in Solids, sponsored by NASA, NBS, and USAF/ASD, San Francisco, Calif., Mar 4-6, 1964

4. R. L. Olson, L. A. McKellar, and W. E. Spicer, <u>The Energetics of Ultraviolet Radiation Damage to White Surfaces</u>, Lockheed Missiles & Space Company, Sunnyvale, Calif., Mar 196

5. "Coatings for the Aerospace Environment," Symposium sponsored by WADC, WADC TR 60-773, Wright Air Development Center, Wright-Patterson Air Force Base, Ohio

6. R. E. Gaumer, F. J. Clauss, M. E. Sibert, and C. C. Shaw, "Materials Effects in Spacecraft Thermal Control," <u>Proceedings, WADD Conference on Coatings for Aerospace Environment</u>, Dayton, Ohio, Nov 1960; WADD TR 60-773

7. W. F. Carroll, <u>Development of Stable Temperature Control Surfaces for Spacecraft — Progress Report No. 1</u>, JPL Technical Report 32-340, Jet Propulsion Laboratory, Pasadena, Calif., Nov 1962

8. G. A. Zerlaut, Y. Harada, and E. H. Tompkins, "Ultraviolet Irradiation in Vacuum of White Spacecraft Coatings," Symposium on Thermal Radiation of Solids sponsored by NASA, ES, and USAF/ASD, San Francisco, Calif., Mar 4-6, 1964

9. H. H. Hormann. <u>Improved Organic Coatings for Temperature Control in a Space Environment</u>. ASD-TDR-62-917. Aeron. Systems Division, USAF, Feb 1963

10. James H. Weaver, <u>Anodized Aluminum Coatings for Temperature Control of Space Vehicles</u>. ASD-TDR-62-918. Aeron. Systems Division, USAF, Feb 1963

11. N. Z. Searle, J. H. Daniel. R. C. Hirt. P. A. Mullen, and W. J. Stehman, <u>Pigmented Surface Coatings for Use in the Space Environment</u>, Report ML-TDR-64-314. Air Force Materials Laboratory, Wright-Patterson AFB, Ohio, Nov 1964

12. E. R. Streed and C. M. Beveridge, "The Study of Low Solar Absorptance Coatings for a Solar Probe Mission," Symposium on Thermal Radiation in Solids Sponsored by NASA, NBS, and USAF/ASD. San Francisco, Calif., Mar 4–6, 1964

13. C. B. Neel. "Measurement of Thermal Radiation Characteristics of Temperature Control Surfaces During Flight in Space," Ninth National Aerospace Instrumentation Symposium. San Francisco, May 1963

14. B. P. Pearson. Jr.. "Preliminary Results From the Ames Emissivity Experiment," AIAA Thermophysics Specialists Conference, Monterey. Calif., Sep 1965

15. Lockheed Missiles & Space Co.. <u>Solar-Radiation-Induced Damage to Optical Properties of ZnO-Type Pigments</u>, LMSC M-50-65-2, 1965

6. J. S. Blakemore. "A Model for Extraterrestrial Solar Degradation of Zinc Oxide." IEEE Transactions on Aerospace and Electronic Systems, Vol. AES-2, Number 3, May 1966. pp. 332–336

17. H. F. MacMillan, A. F. Sklensky. and C. A. McKellar, "Apparatus for Spectral Bidirectional Reflectance Measurements During Ultraviolet Irradiation in Vacuum." AIAA Progress in Aeronautics and Astronautics, Vol. 18. pp. 129–149, Academic Press 1966

18. R. H. Bube. "Mechanism of Photoconductivity in Microcrystalline Powders." J. Appl. Phys. 31, 12 (1960)

19. E. E. Hahn, "Some Electronic Properties of Zinc Oxide Semiconductor," J. Appl. Phys. 22, 855 (1951)

20. G. Heiland, E. Mollwo, and F. Stöckmann, "Electronic Processes in Zinc Oxide," Solid State Physics, Vol. 8, Academic Press, 1959

21. R. J. Collins and D. G. Thomas, "Photoconduction and Surface Effects With Zinc Oxide Crystals," Phys. Rev. $\underline{112}$, 2 (1958)

22. D. B Medved, "Photodesorption in Zinc Oxide Semiconductor," J. Chem. Phys. $\underline{28}$, 870 (1958)

23. V. N. Filimonov, "Electronic Absorption Bands of ZnO and TiO_2 in the Infrared Region of the Spectrum," Optika i Spektr $\underline{5}$, 709 (1958)

24. IIT Research Institute, Stable White Coatings, IITRI-U6004-21 (1966)

25. E. A. Schatz, "Effect of Pressure on the Reflectance of Compacted Powders," J. Opt. Soc. Am. $\underline{56}$, 3 (1966)

26. E. Scharowsky, "Optical and Electronic Properties of ZnO Single Crystals With Zn Additions," Z. Physik $\underline{135}$ 318 (1958)

27. D. G. Thomas, "Interstitial Zinc in Zinc Oxide," J. Phys. Chem. Solids $\underline{3}$, (1957)

28. J. Schneider and A. Räuber, Z. Naturforsch. $\underline{16a}$, 713 (1961)

29. P. Kasai, Phys. Rev. $\underline{130}$, p. 989 (1963)

30. K. A Müller and J. Schneider, Physics Letters $\underline{4}$, 288 (1963)

31. R. J. Kokes, J. Phys. Chem. $\underline{66}$, 99 (1962)

32. Baranov, E. V., Kholmogoro V.E., and Terenin, A. N., Dokl. Phys. Chem. $\underline{146}$, 125 (65)

33. C. H Geisler and G. J. Simmons, Physics Letters $\underline{11}$, 111 (1964)

34. K. M. Sancier, ESR Investigation of Gas-Solid Interaction, J. Catalysis $\underline{5}$, 314 (1966)

35. R. L. Weiher, Optical Properties of Free Electron in ZnO Phys. Rev. $\underline{152}$, 152 (1966)